JPL Publication 82-69, Addendum 1

Solar Cell Radiation Handbook

Addendum 1: 1982-1988

B. E. Anspaugh

February 15, 1989

NASA
National Aeronautics and
Space Administration

Jet Propulsion Laboratory
California Institute of Technology
Pasadena, California

The research described in this publication was carried out by the Jet Propulsion Laboratory, California Institute of Technology, under a contract with the National Aeronautics and Space Administration.

ABSTRACT

This is the first in a series of updates to the Solar Cell Radiation Handbook (JPL Publication 82-69). In order to maintain currency of solar cell radiation data, recent solar cell designs have been acquired, irradiated with 1 MeV electrons, and measured. The results of these radiation experiments are reported in this publication.

ACKNOWLEDGEMENTS

The author wishes to express his appreciation to Robert Weiss who was responsible for carrying out all the irradiations and laboratory measurements reported in this publication, and to Ram Kachare who researched the detailed technical information on the materials properties of the compound semiconductors.

TABLE OF CONTENTS

TABLES

FIGURES

FIGURES (Continued)

I. INTRODUCTION

This is the first in a series of addenda to the Solar Cell Radiation Handbook[1]. Since the last revision of the Handbook was issued, many new developments in solar technology have come forth. In silicon cell technology, improvements in cell manufacturing have been generally based on refining and automating many of the manufacturing procedures. For example, the dual antireflection (AR) coating, which was once an optional item, has become standard -- back surface fields, which were once always formed by using an aluminum paste print-on technique, are now commonly formed by using boron. The back surface reflector, formed by evaporating a reflective coating on the rear cell surfaces, is now included in the "base price" and is no longer really an option.

Cells have been made with gridded-back contacts for use on thin, semi-transparent substrates to allow the unuseable infrared portion of the solar spectrum to pass through without raising the temperature. Cells have also been made with the front contacts wrapped around and over the cell edge so that both terminals are available for more convenient electrical connection from the back side only. As a refinement to the wraparound technique, some cells have even been made with holes drilled through, from front to back, and the contacts wrapped through to the back.

The average thickness of flight solar cells has decreased over the years, and it is now rather uncommon to see cells flown that are thicker than 200 μm. Cells as thin as 100 μm are being flown more and more often, and cells as thin as ~60 μm have been used on at least one flight program. The average size of flight cells has increased since the last edition of the Handbook was produced. In the early 80's, 2 x 2 cm solar cells were still in common use,

but now, they have almost disappeared from panel assembly lines, replaced by 2 x 4 cm cells. Additionally, 2 x 6 cm cells have been flown, and 4 x 4 and 8 x 8 cm cells are rapidly coming onto the scene.

Experimental solar cells with considerably increased cell efficiencies have been made on an experimental basis in the laboratory. Techniques such as dot contacts, which minimize the contact area between silicon and the metallization, and passivation layers between the silicon front surfaces and the front contacts have been effective in increasing efficiencies. Preliminary results indicate that the radiation tolerance of such cells can be quite acceptable. Although none of these techniques have found their way onto production lines, it is likely that they may become standard techniques in the near future.

The overall result is that the character of silicon cells has changed considerably over the past few years. Cells are made with a whole host of new techniques and are now commonly made with higher efficiencies and with much more consistent electrical performance than they were in the very recent past. But how did they behave in radiation? The new cells differ sufficiently from their predecessors so that the old radiation data on cells of the same functional description may be badly misleading.

A lot of progress has been made on cells constructed from materials other than silicon. In particular, gallium arsenide (GaAs) technology has received a lot of attention during the last few years. As a material, GaAs has been attractive to solar cell workers for a long time because of its potential for producing cells which have higher efficiencies, are capable of operating at high temperatures, have high radiation resistance. Since GaAs is a direct

bandgap material with a high light-absorption coefficient, GaAs cells also have the very desirable potential of being made very thin.

At the time the Handbook was published, the only GaAs devices available in quantity that had the physical characteristics of flyable solar cells were the cells made by Hughes Research Laboratories using the liquid phase epitaxy (LPE) method. The Hughes workers achieved several technological breakthroughs in developing their cells, among which were practical AlGaAs windows, metal contact systems, and antireflection coatings. The radiation characteristics of these cells were reported in the 1982 Handbook. Since that time, other companies have entered the GaAs arena, mostly using the organo-metallic chemical vaporization deposition (OMCVD) process. Several companies have brought these cells to production readiness and at least one company has delivered several thousand GaAs cells for a flight program. Up until recently, most GaAs cells have been grown on GaAs substrates. Although GaAs cells only have to be a few tens of microns thick because the light-absorption coefficient is so high, it has been impractical to produce cells much thinner than ~300 μm because GaAs is somewhat fragile. Therefore, a substantial amount of effort has gone into finding an alternate substrate which is cheaper, lighter, more robust, and has the right lattice match to allow growth of GaAs. Germanium (Ge) appears to fulfill most of these requirements, and recently GaAs/Ge cells have been successfully produced.

Materials other than GaAs have received attention also. Most of these materials have high light-absorption coefficients, so that their solar cells can be made very thin and, consequently, these materials are commonly referred to as thin film materials. Examples are indium phosphide (InP),

amorphous silicon (a-Si), and copper indium diselenide on cadmium sulfide ($CuInSe_2/CdS$).

InP has a bandgap of 1.35 eV at 300K and light-absorption coefficients of $>10^4$/cm for photon energies above bandgap energy. Thin film InP cells have reportedly been made with air mass zero (AM0) efficiencies as high as 17%. These cells have been shown to be quite resistant to radiation damage.

Amorphous silicon has an effective bandgap energy of about 1.6 eV and cells made of this material have been measured at JPL which have AM0 efficiencies of about 8%. Amorphous silicon solar cells have been irradiated with both protons and electrons. Although a-Si solar cells exhibit a substantial amount of radiation damage under both proton and electron bombardment, most of the damage appears to anneal out at temperatures less than 200°C. The main difficulty with a-Si cells is that they exhibit a severe instability when exposed to light over extended periods of time.

$CuInSe_2$ (CIS for short) has a bandgap of 1.04 eV, and CdS has a bandgap energy of 2.7 eV. A limited number of CIS cells made with special test contacts were furnished to JPL by ARCO. AM0 efficiencies of these cells when corrected for the presence of the contacts were nearly 10%. Some preliminary electron irradiation results at JPL have shown these cells to be very radiation resistant to fluences as high as 5×10^{16} e/cm^2, but radiation results on other cells indicate that CIS cells may be easily damaged by low energy protons. There is no reported photon degradation of $CuInSe_2$ cells, and it is proving to be a very interesting material for possible future solar cell applications.

II. TREATMENT OF RADIATION INCIDENT FROM THE REAR

In building modern solar panels, most solar array design engineers attempt to build panels which maximize the power/mass ratio. Many designs are beginning to incorporate light, flexible substrates in order to decrease the mass. This leaves the rear surfaces of the cells much more vulnerable to radiation. A proton irradiation program was carried out at JPL with the objective of assessing solar cell damage induced by rear-incident protons[2]. Normal and omnidirectional incidence were used to irradiate both BSF and non-BSF cells of two different thicknesses. The data were used to compute damage coefficients appropriate for rear-incident radiation. It was found that the bulk area of the solar cells provided a certain amount of self-shielding, which essentially protected the junction area from rear-incident radiation. It was found that as the cell thickness decreased, the self-shielding effect decreased. For example, 75-μm-thick non-BSF cells offered an equivalent self-shielding thickness of 50 μm, while similar 200-μm-thick cells provided a self-shielding thickness of 100 μm.

Cells incorporating back surface fields were much more vulnerable to back surface radiation. Low energy protons have ranges which cause them to stop in the field region where they apparently cause a lot of damage because the cell electrical parameters die away at much lower fluences than they do for non-field cells. Here it was found that 75-μm-thick BSF cells offered equivalent self-shielding thicknesses of only 12 μm, while 200-μm-thick BSF cells provided self-shielding thicknesses of 50 μm. These results are summarized in Table 1.

Note that these thicknesses apply only to the self-shielding of the solar cells themselves, including the usual 5 μm thickness of silver used in the

Table 1. Equivalent Shielding Thicknesses for Rear Cell Surfaces

Cell Type	Equivalent Thickness (μm)
non-BSF 75 μm	50
non-BSF 200 μm	100
BSF 75 μm	12
BSF 200 μm	50

rear contacts. Additional shielding due to the substrate thickness and adhesive (if any) should be added to the above numbers to account for the total amount of shielding of the rear cell surfaces. The substrate and adhesive thicknesses should be converted to equivalent quartz thicknesses using a density correction. That is, a 200 μm substrate with half the density of quartz would be counted as a 100-μm-thick shield. After conversion to equivalent quartz thicknesses all the rear shield thicknesses are additive.

The total 1 MeV equivalent fluence for the coverglass/cell/substrate combination is computed by assuming half the fluence is incident on the front of the cell and half is incident on the rear. Compute, using the EQFRUX program, the 1 MeV equivalent electron fluences for all eight coverglass thicknesses. Find the equivalent fluence for the front coverglass, interpolating if necessary. Find the equivalent fluence for the rear shielding, again interpolating if necessary. Since EQFRUX calculates the equivalent fluence as though the cells were protected by infinite backshielding, the equivalent fluences as found above for the front and for the rear may be added together without further correction. This becomes the total equivalent fluence for the panel degradation, and the behavior of the specific cell parameters may be found either from the appropriate curves in this publication, in the Handbook, or elsewhere.

III. 1 MeV SOLAR CELL IRRADIATIONS

Many of these newer solar cells have been acquired and irradiated with 1 MeV electrons. However, for this first Addendum, we have concentrated our attention on Si and GaAs cells, particularly those in current production. In the Si cell area, we have acquired cells which the solar cell manufacturers judged would be of the most interest to their customers. The cells reported on include two types which are 8 mils (200 μm) thick. The first type consists of 10 ohm-cm cells with back surface fields (BSF) and back surface reflectors (BSR). The second type consists of 2 ohm-cm cells with BSRs, but no BSFs. The third type includes 10 ohm-cm cells with boron BSFs, BSRs, and gridded back contacts. The gridded-back contacts were used in these cells to reduce cell bowing, which occurs in thin cells with full metal coverage. Cells in the third group were separated into three thickness ranges: 2.6 to 3.1 mils, 3.3 to 3.4 mils, and 3.5 to 3.6 mils. This grouping enabled a test of thin cell radiation susceptibility with thickness as a parameter.

We are reporting on one of the newer types of GaAs solar cells where the GaAs is deposited by the OMCVD process onto a germanium substrate. This type of structure is commonly referred to as GaAs/Ge. These cells are made by first depositing an n-type buffer layer ~8 μm thick onto the Ge, followed by deposition of a p-layer ~0.45 μm thick. The n-layer is doped with Se to a concentration of about 6×10^{17} and the p-layer is doped with Zn to a concentration of 2 to 3×10^{18}. An AlGaAs window ~600 Angstroms thick is added, then a dual AR coating consisting of TiO_x and Al_2O_3. The front contacts are made of Au, Zn, Au, and Ag and the rear contacts are made of Au, Ge, Ni, Au, and Ag.

No suitable GaAs/GaAs cells were available for irradiation as of this writing, so we will defer reporting on those cells until the next edition. However, we have made a few spot checks of the degradation of recent GaAs/GaAs cells and compared them with GaAs/Ge cells. The behavior of the two types of cells has been seen to be essentially identical, and the GaAs/Ge data can be used for both types of cells coming from the ASEC firm.

The radiation data are presented in plots identical to the format used in the Solar Cell Radiation Handbook. We have plotted current density and power density in units of ma/cm^2 or mW/cm^2, where the total cell size, including contacts and busbar, has been used in computing the area. The plots include both absolute cell values and values normalized to their readings before radiation. The cell data are plotted in Figures 1 to 30 according to the following schedule.

Table 2. Cell Plots vs. Figure and Page Nos.

Cell Description			Figure Nos.	Page Nos.
Si 2 ohm-cm BSF	8 mils	2 x 4	1 - 10	0 - 19
Si 10 ohm-cm BSFR	8 mils	2 x 2	1 - 10	10 - 19
Si 10 ohm-cm BSFR	2.6 - 3.1 mils	2 x 4	11 - 20	20 - 29
Si 10 ohm-cm BSFR	3.3 - 3.4 mils	2 x 4	11 - 20	20 - 29
Si 10 ohm-cm BSFR	3.5 - 3.8 mils	2 x 4	11 - 20	20 - 29
GaAs/Ge		2 x 4	21 - 30	30 - 39

IV. REFERENCES

1. H. Y. Tada, J. R. Carter, Jr., B. E. Anspaugh, and R. G. Downing, Solar Cell Radiation Handbook, JPL Publication 82-69, Jet Propulsion Laboratory, Pasadena, California. Nov. 1982.

2. B. E. Anspaugh and R. Kachare, "Effect of Front and Rear Incident Proton Irradiation on Silicon Solar Cells," Conf. Rec. of the 19th IEEE Photovoltaic Specialists Conf., 721 1987.

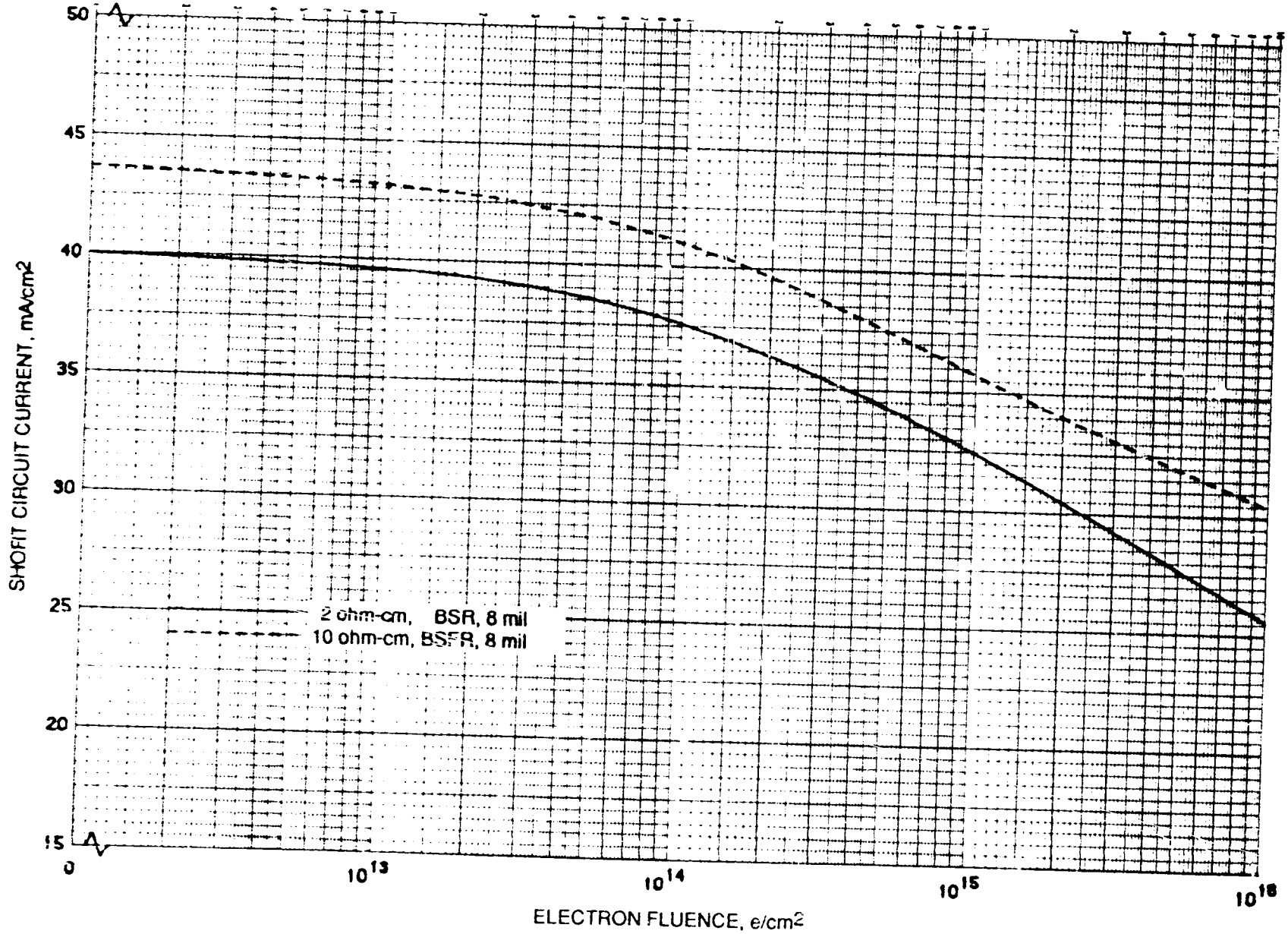

Figure 1. I_{sc} vs. 1 MeV Electron Fluence for Si 2 ohm-cm BSF and 10 ohm-cm BSFR Cells

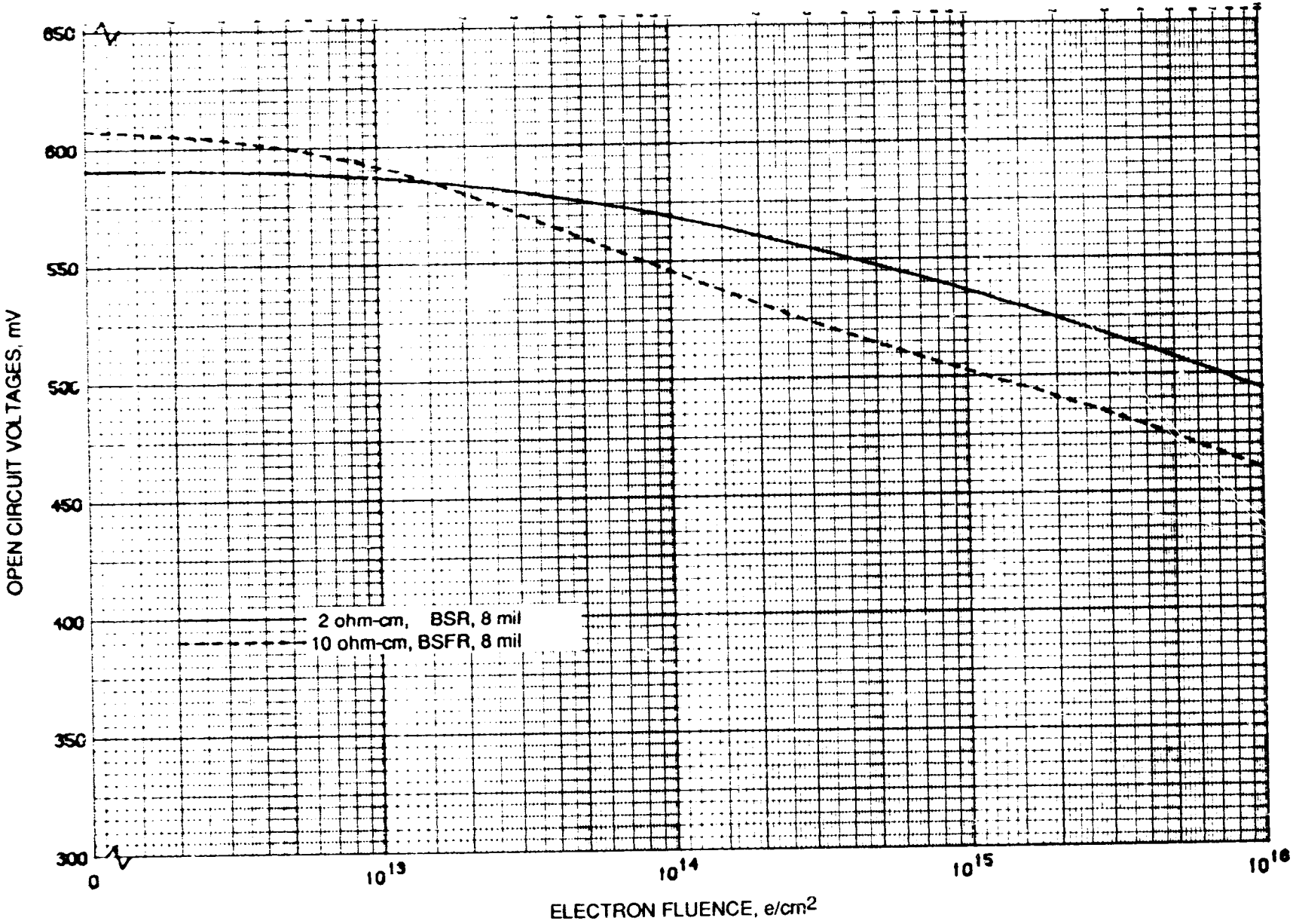

Figure 2. V_{oc} vs. 1 MeV Electron Fluence for Si 2 ohm-cm BSF and 10 ohm-cm BSFR Cells

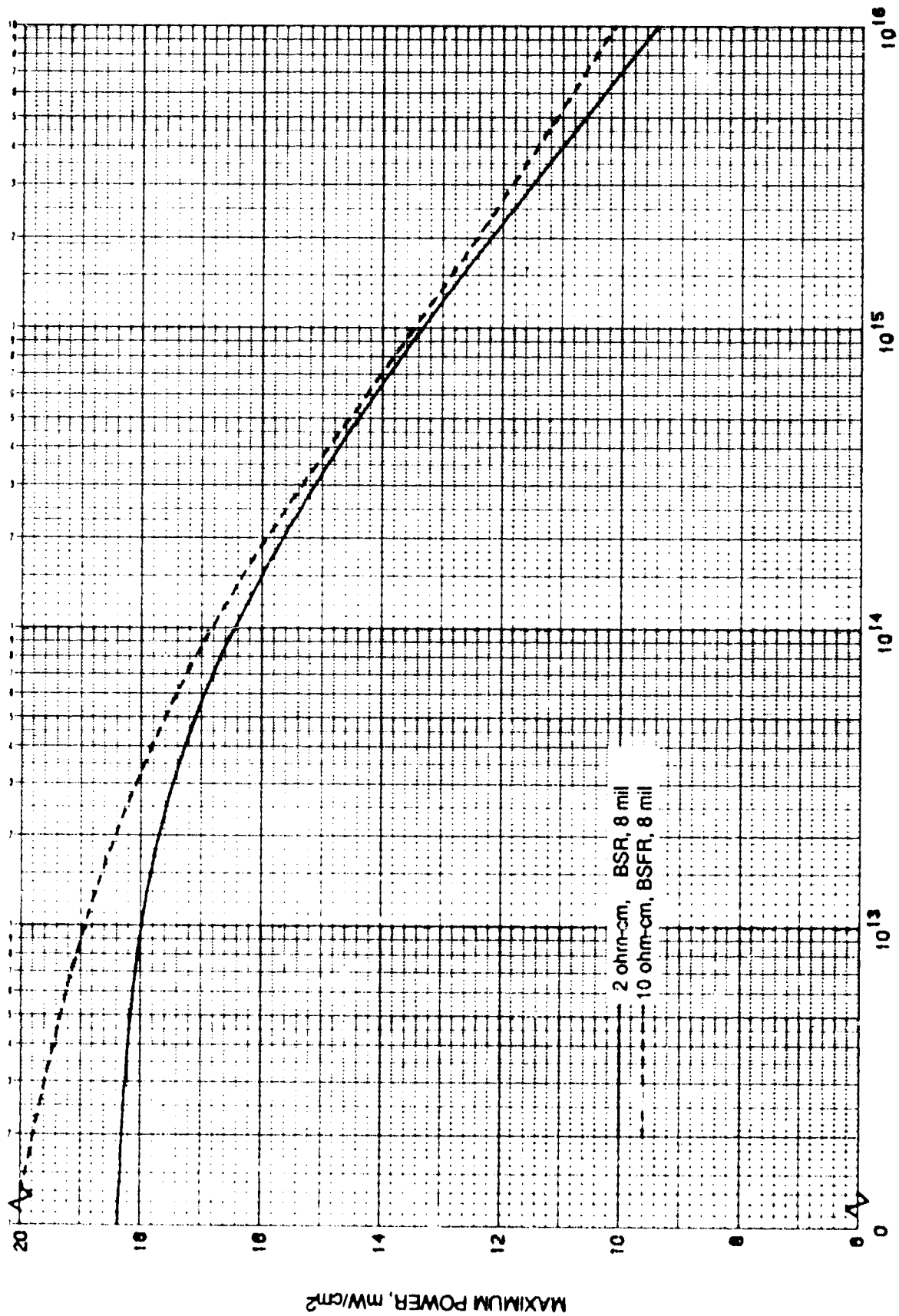

Figure 3. P_{max} vs 1 MeV Electron Fluence for Si 2 ohm-cm BSF and 10 ohm-cm BSFR Cells

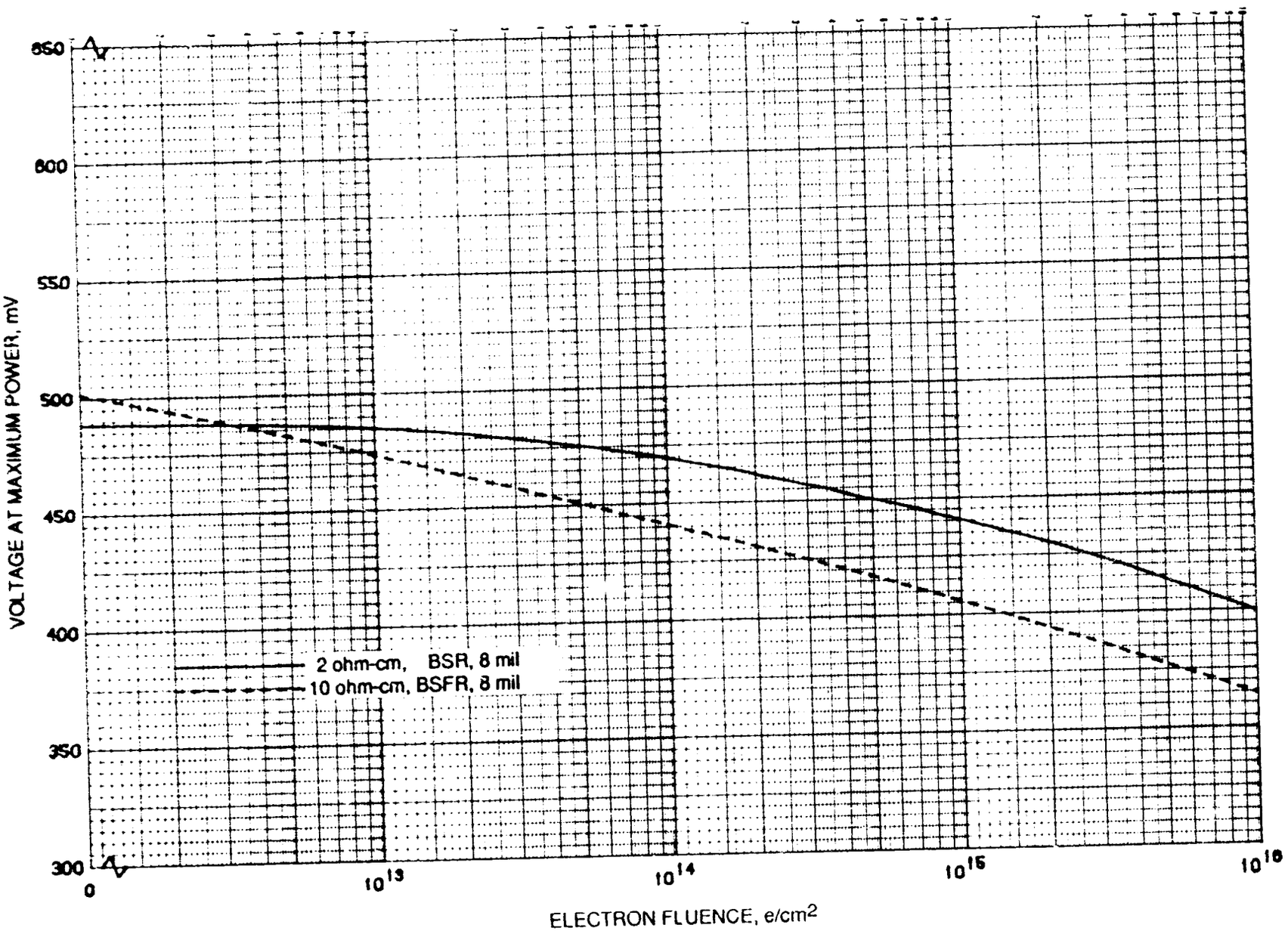

Figure 4. V_{mp} vs. 1 MeV Electron Fluence for Si 2 ohm-cm BSF and 10 ohm-cm BSFR Cells

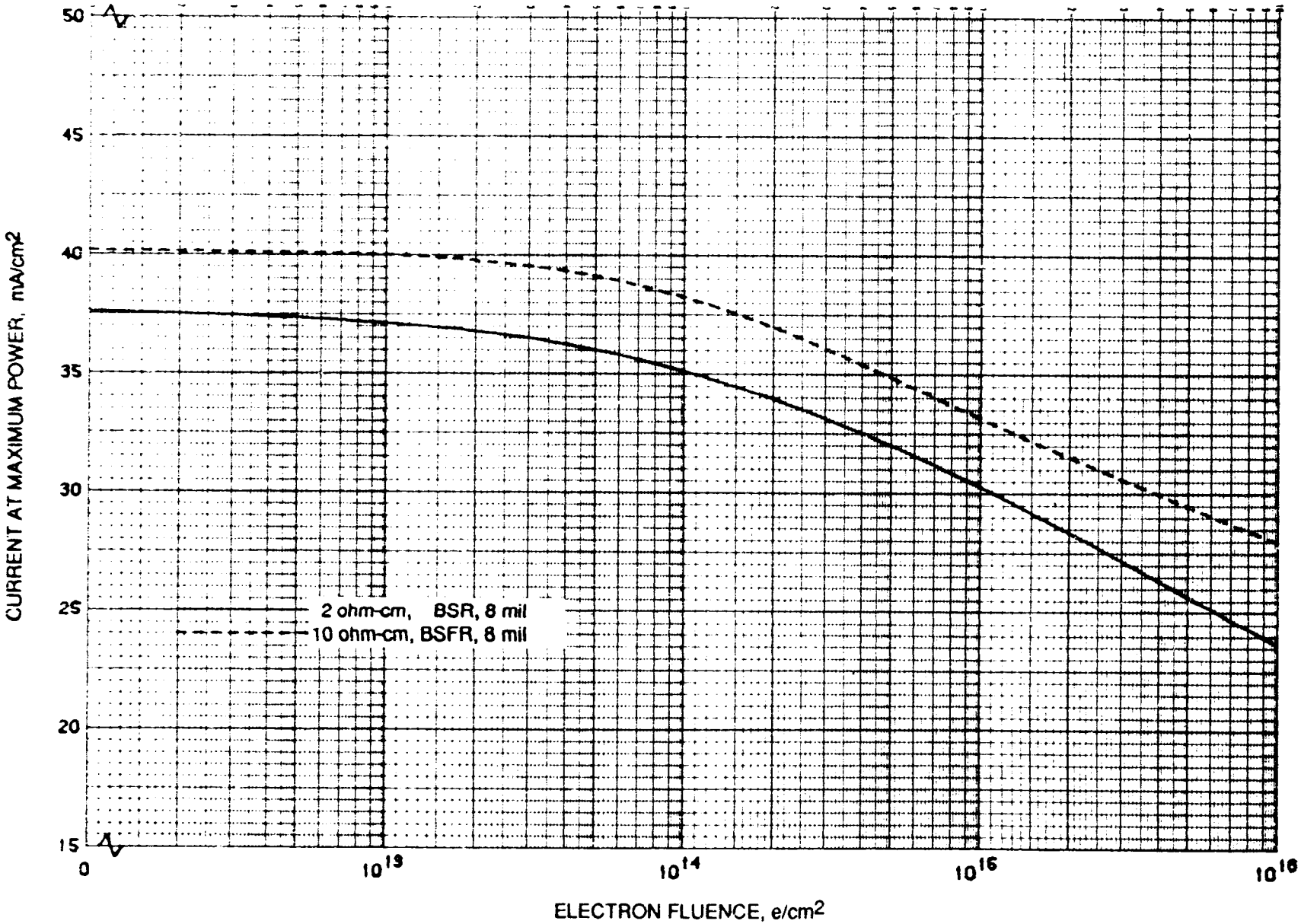

Figure 5. I_{mp} vs. 1 MeV Electron Fluence for Si 2 ohm-cm BSF and 10 ohm-cm BSFR Cells

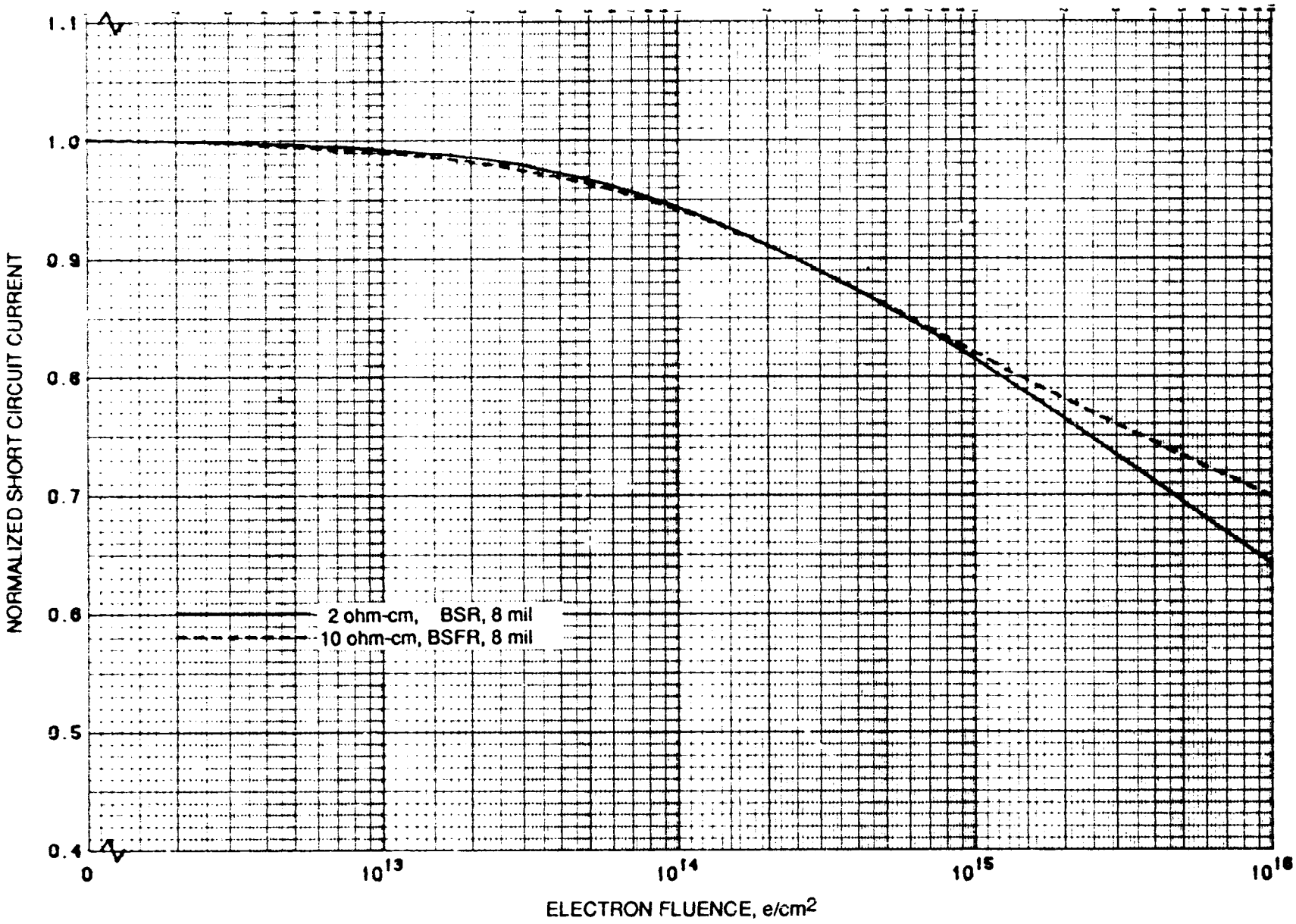

Figure 6. Normalized I_{sc} vs. 1 MeV Electron Fluence for Si 2 ohm-cm BSF and 10 ohm-cm BSFR Cells

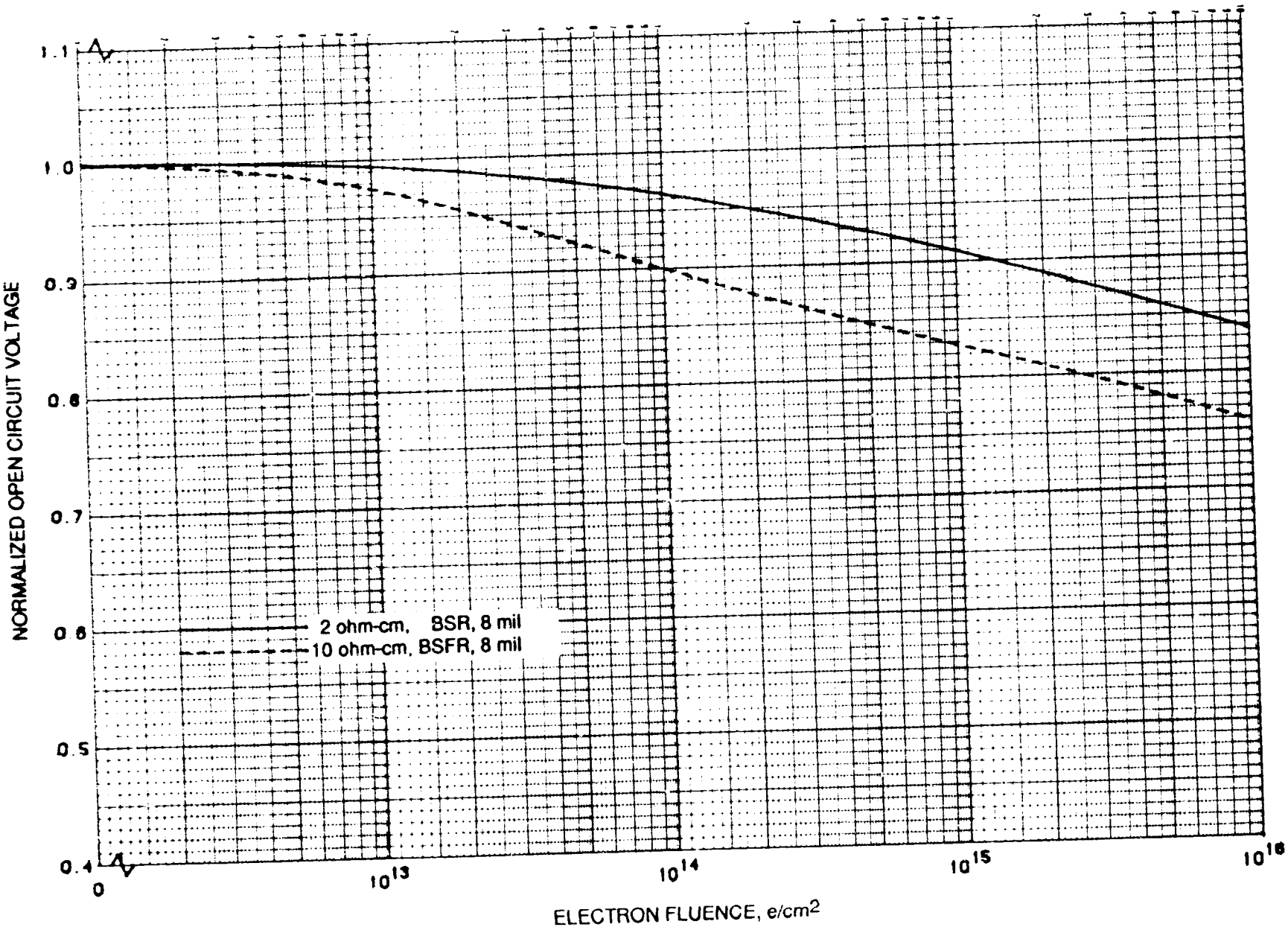

Figure 7. Normalized V_{oc} vs. 1 MeV Electron Fluence for Si 2 ohm-cm BSF and 10 ohm-cm BSFR Cells

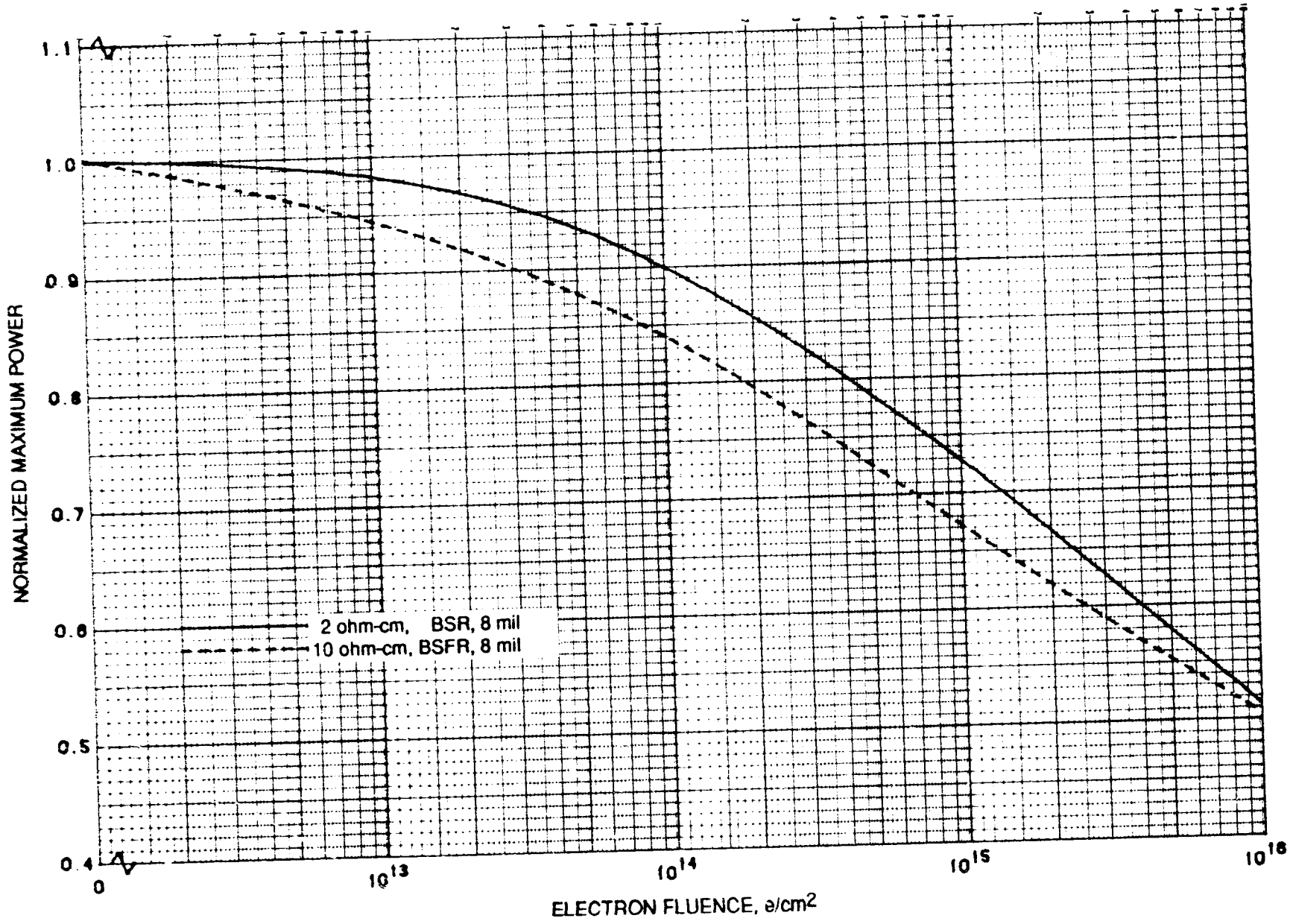

Figure 8. Normalized P_{max} vs. 1 MeV Electron Fluence for Si 2 ohm-cm BSF and 10 ohm-cm BSFR Cells

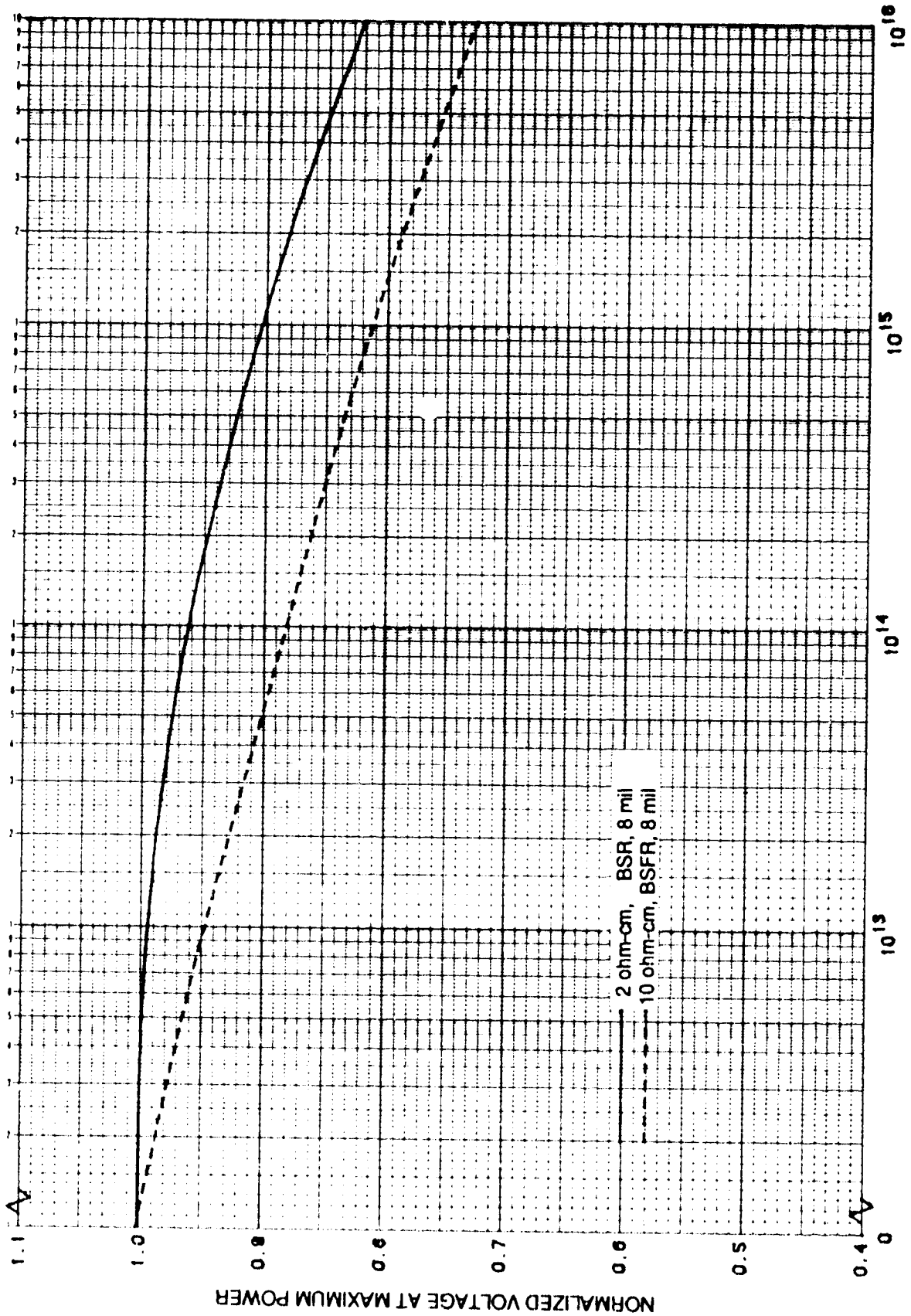

Figure 9. Normalized V_{mp} vs. 1 MeV Electron Fluence for Si 2 ohm-cm BSF and 10 ohm-cm BSFR Cells

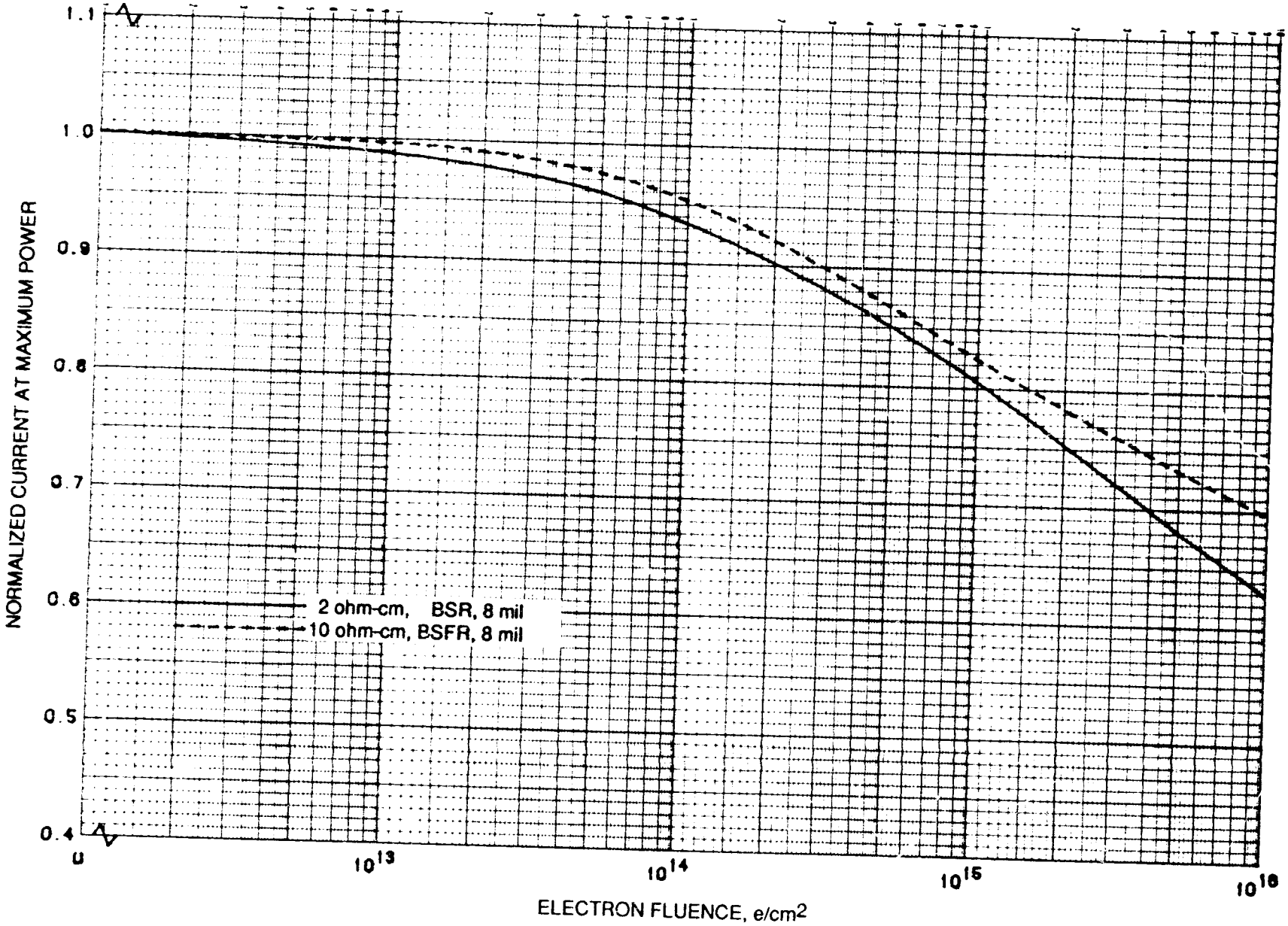

Figure 10. Normalized I_{mp} vs. 1 MeV Electron Fluence for Si 2 ohm-cm BSF and 10 ohm-cm BSFR Cells

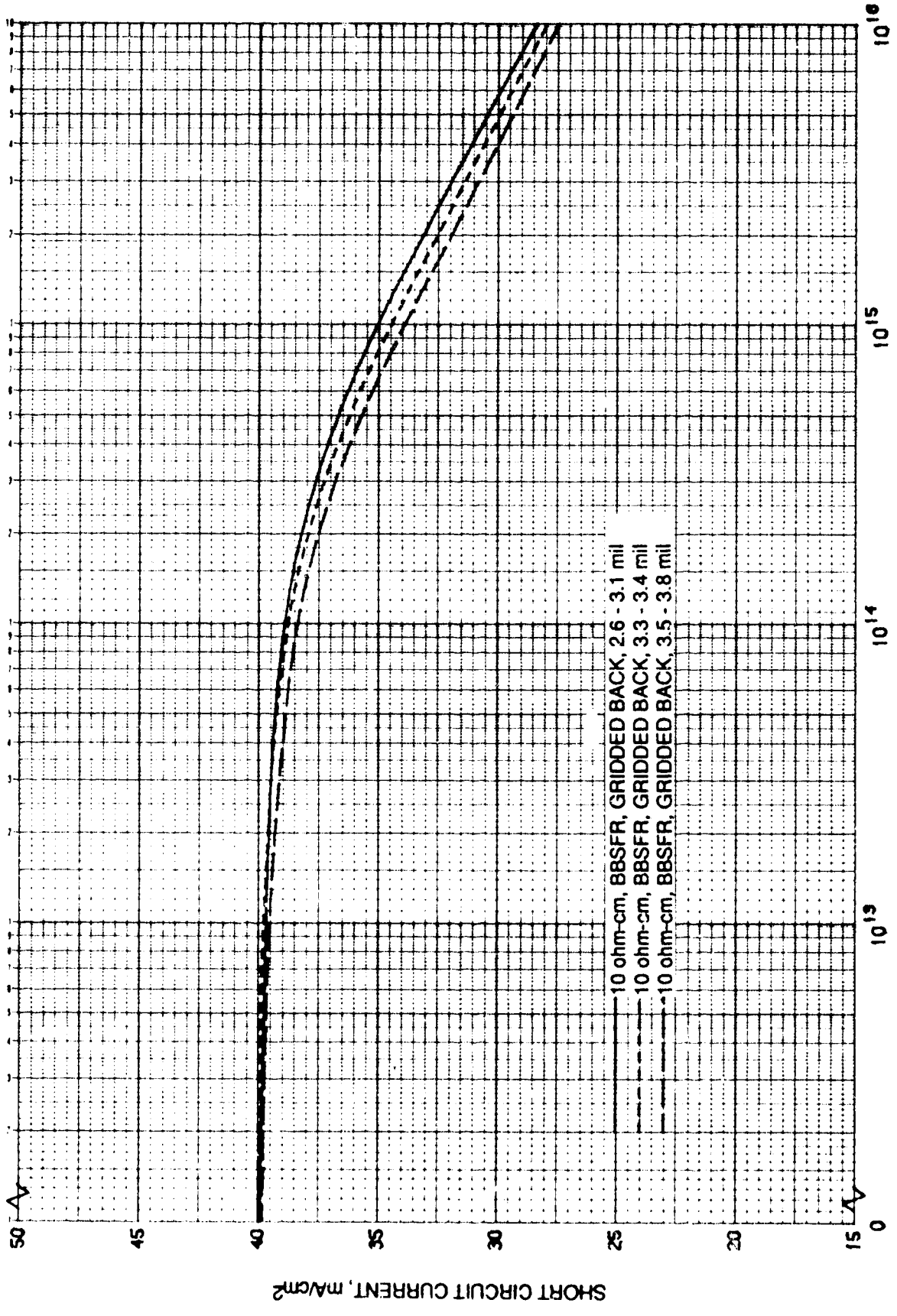

Figure 11. I_{sc} vs. 1 MeV Electron Fluence for Si 10 ohm-cm BSFR Thin Cells (2.6 - 3.1 mils)

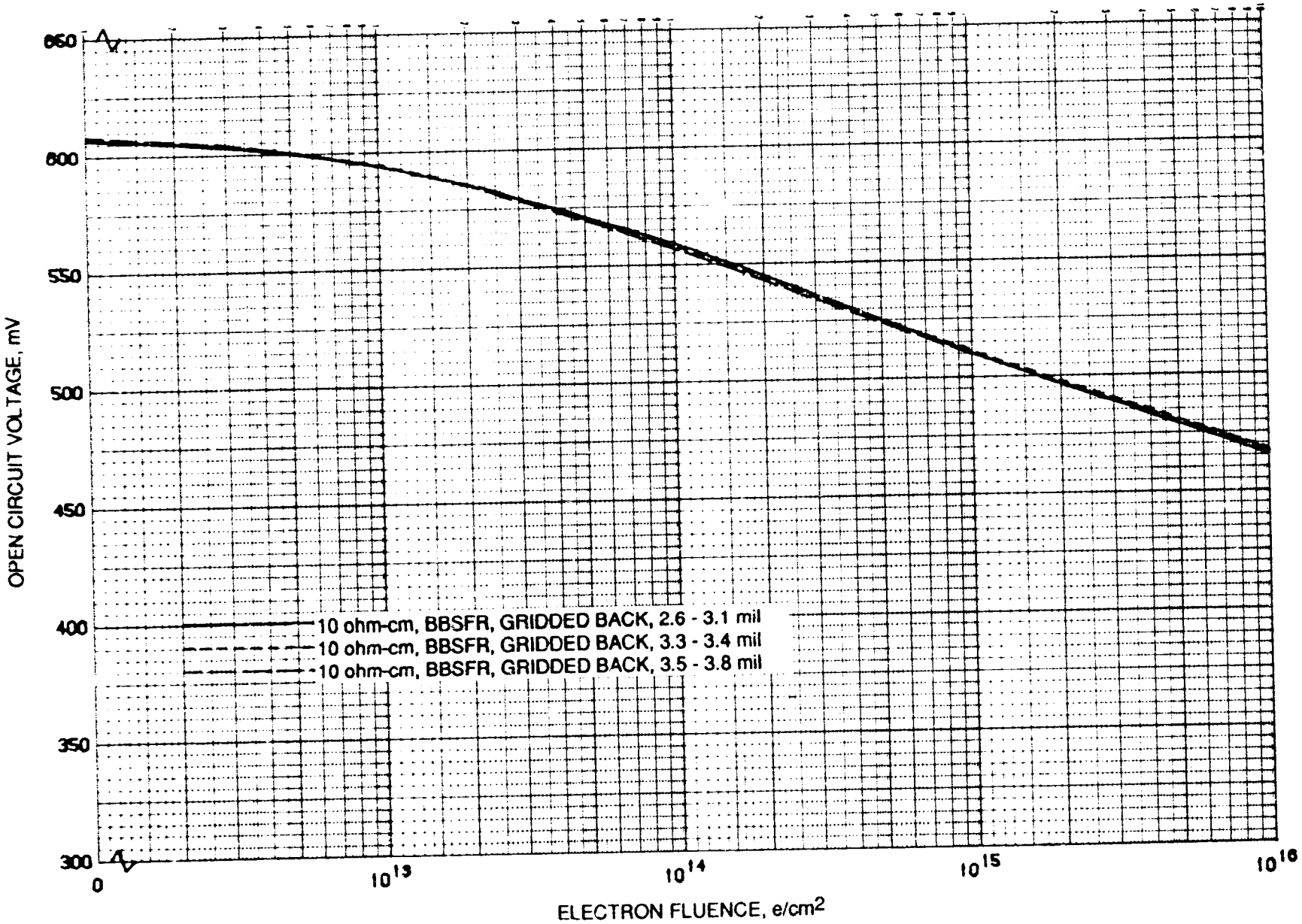

Figure 12. V_{oc} vs. 1 MeV Electron Fluence for Si 10 ohm-cm BSFR Thin Cells (2.6 - 3.1 mils)

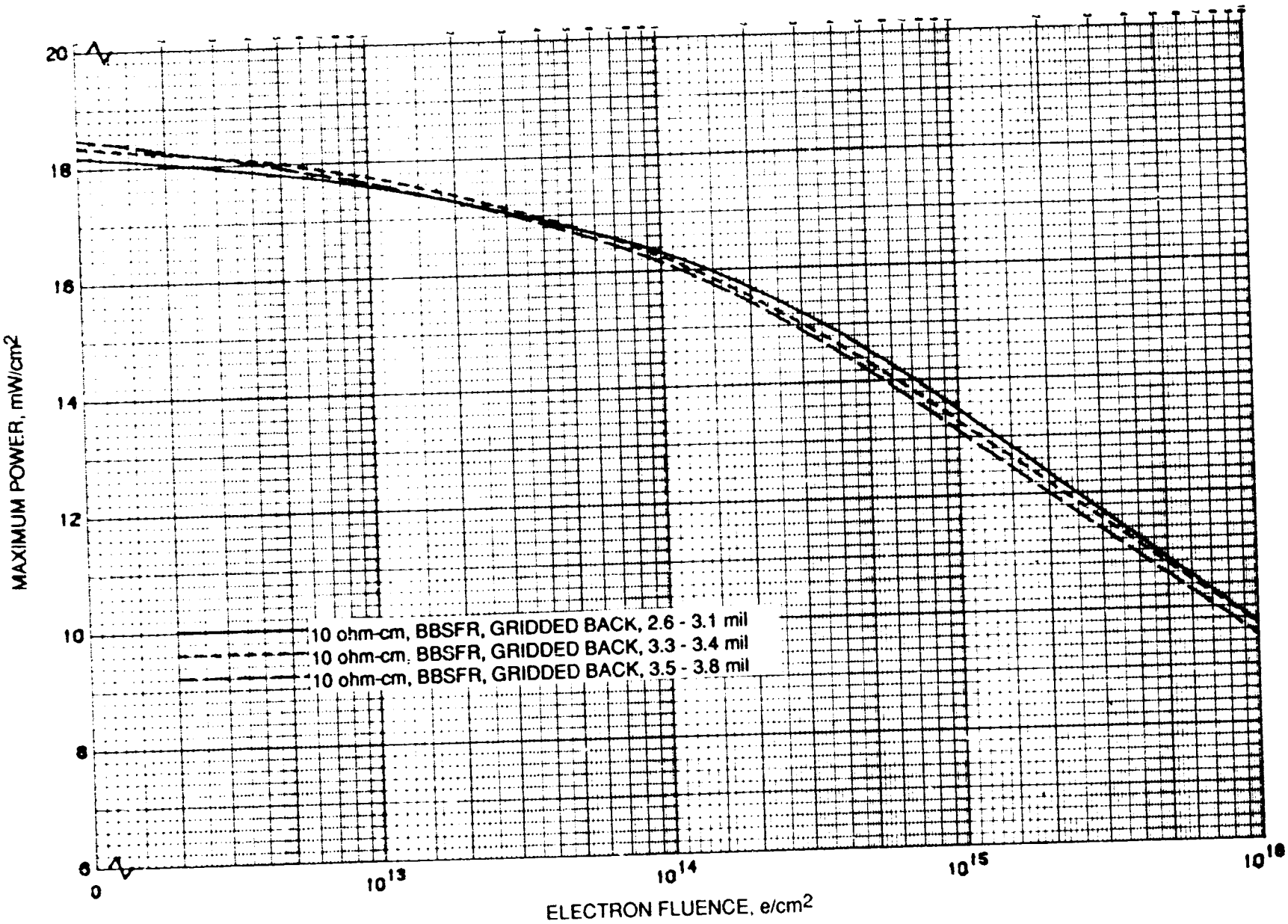

Figure 13. P_{max} vs. 1 MeV Electron Fluence for Si 10 ohm-cm BSFR Thin Cells (2.6 - 3.1 mils)

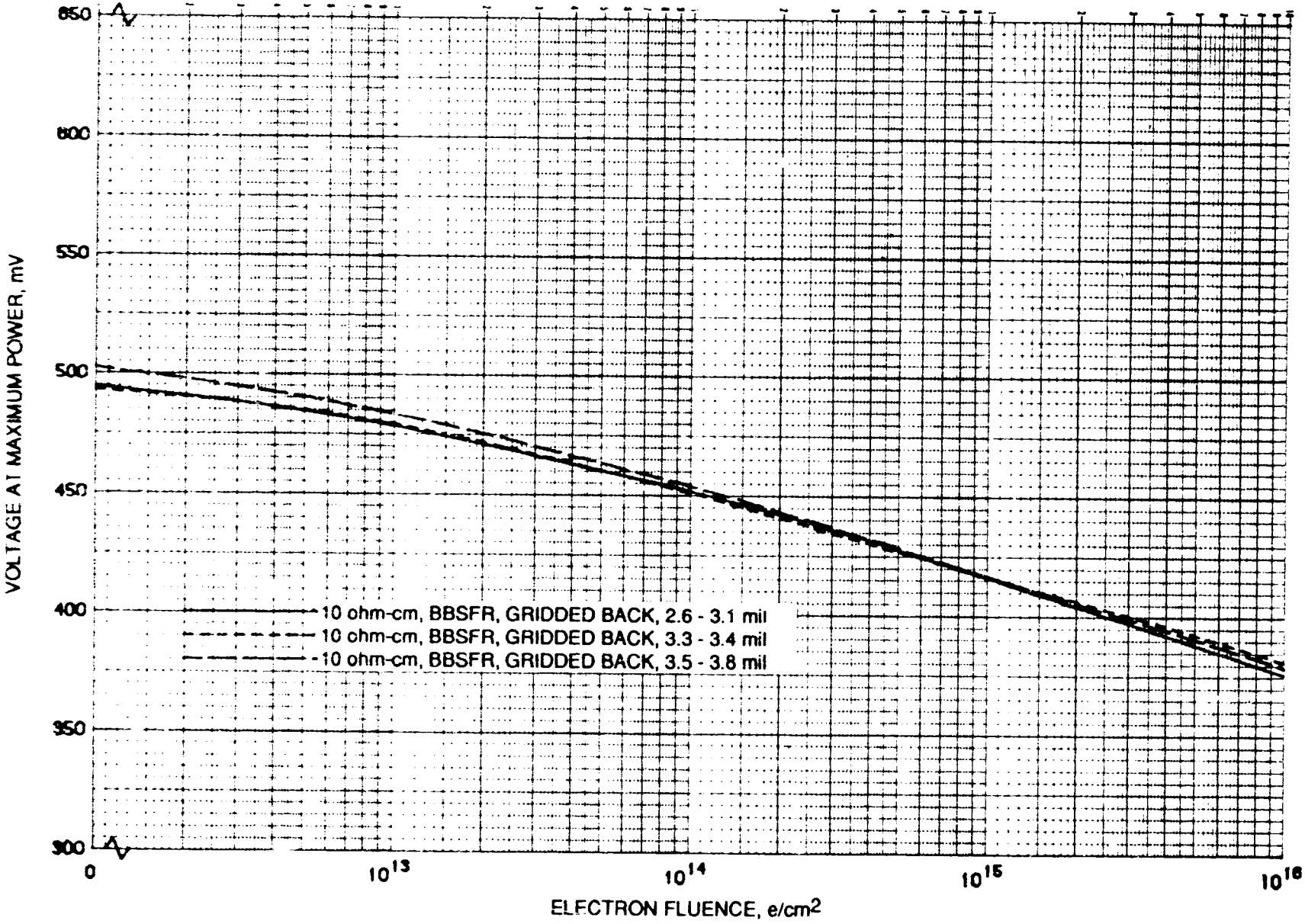

Figure 14. V_{mp} vs. 1 MeV Electron Fluence for Si 10 ohm-cm BSFR Thin Cells (2.6 - 3.1 mils)

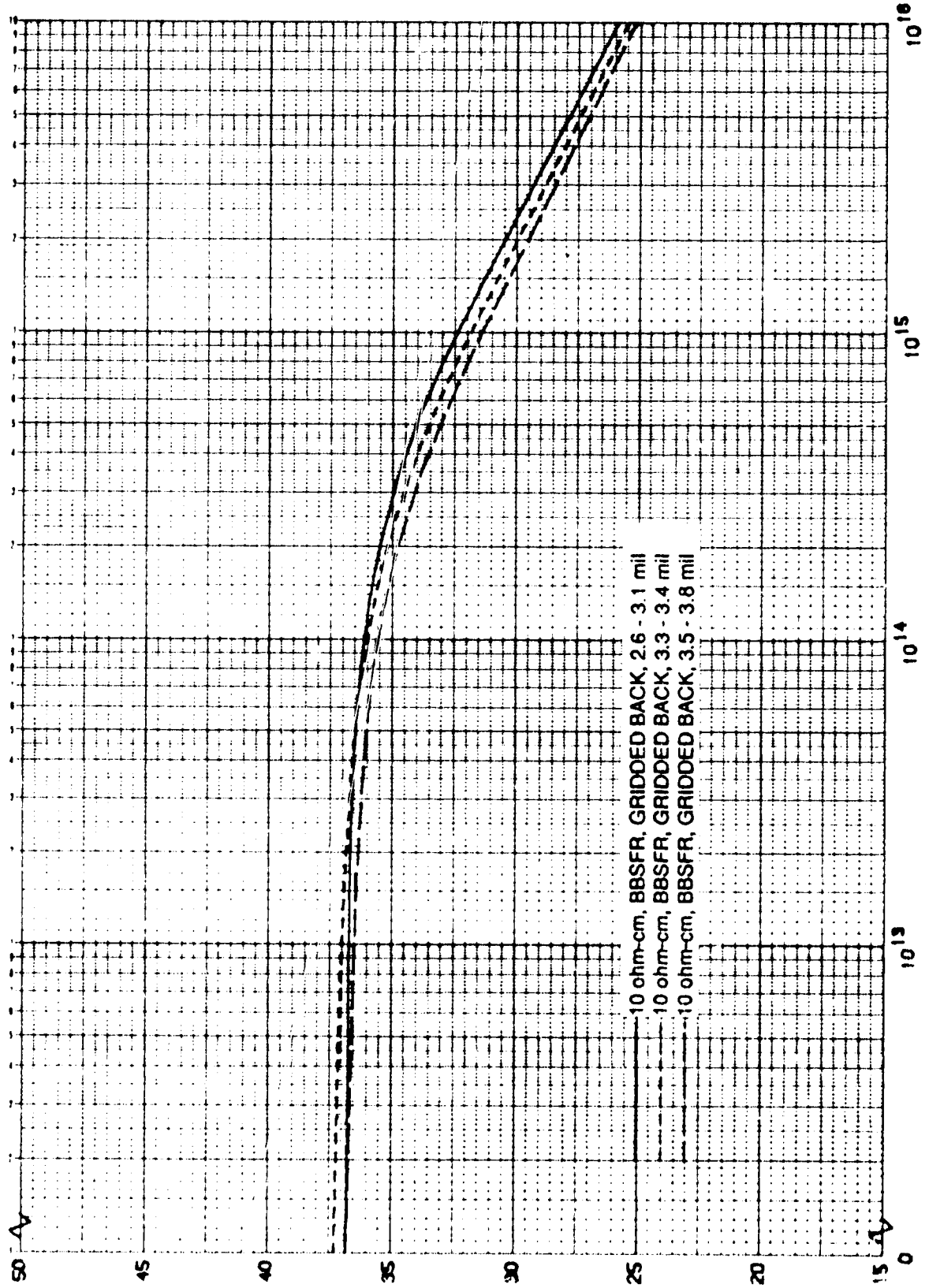

Figure 15. I_{mp} vs. 1 MeV Electron Fluence for Si 10 ohm-cm BSFR Thin Cells (2.6 - 3.1 mils)

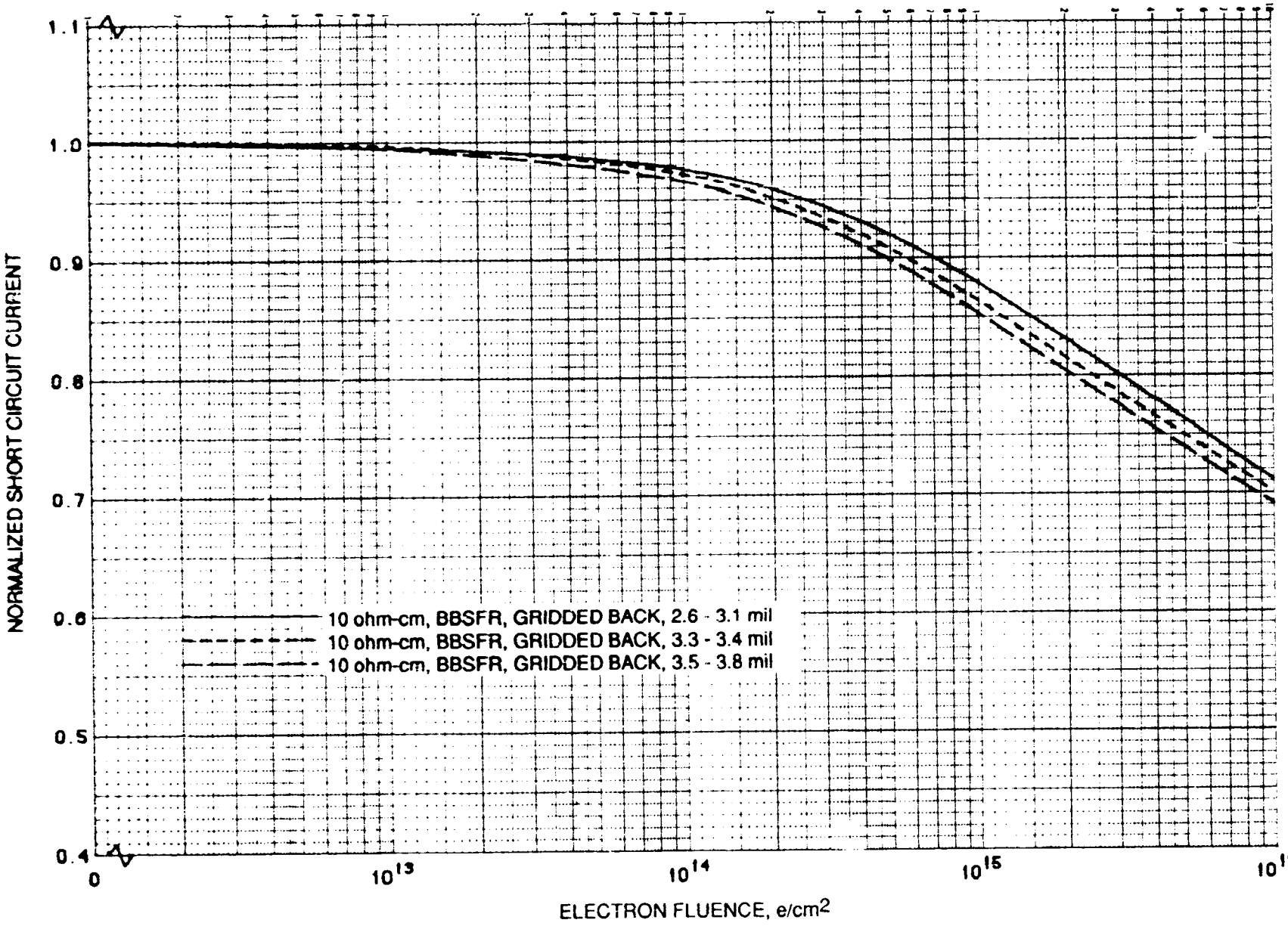

Figure 16. Normalized I_{sc} vs. 1 MeV Electron Fluence for Si 10 ohm-cm BSFR Thin Cells (2.6 - 3.1 mils)

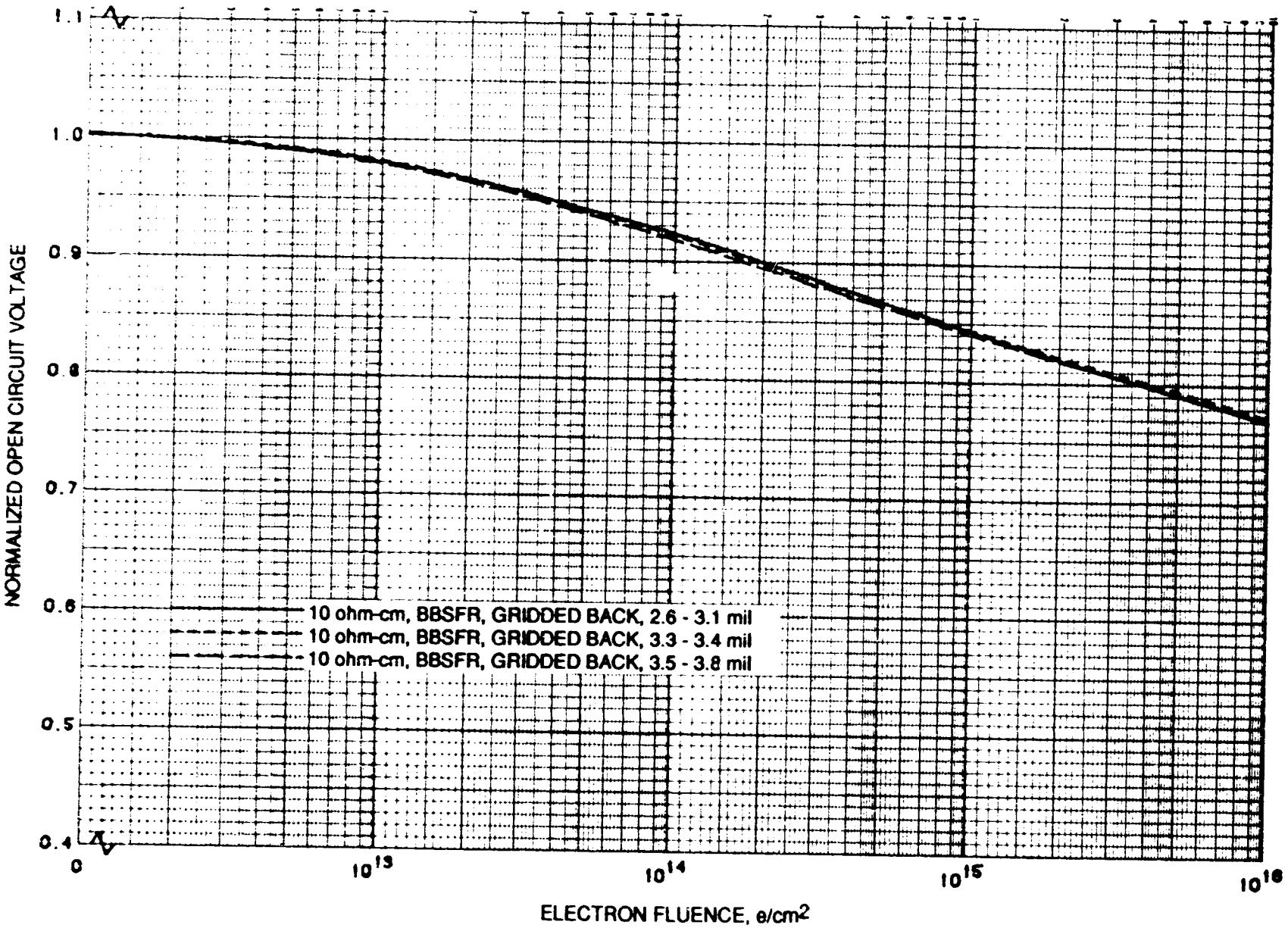

Figure 17. Normalized V_{oc} vs. 1 MeV Electron Fluence for Si 10 ohm-cm BSFR Thin Cells (2.6 - 3.1 mils)

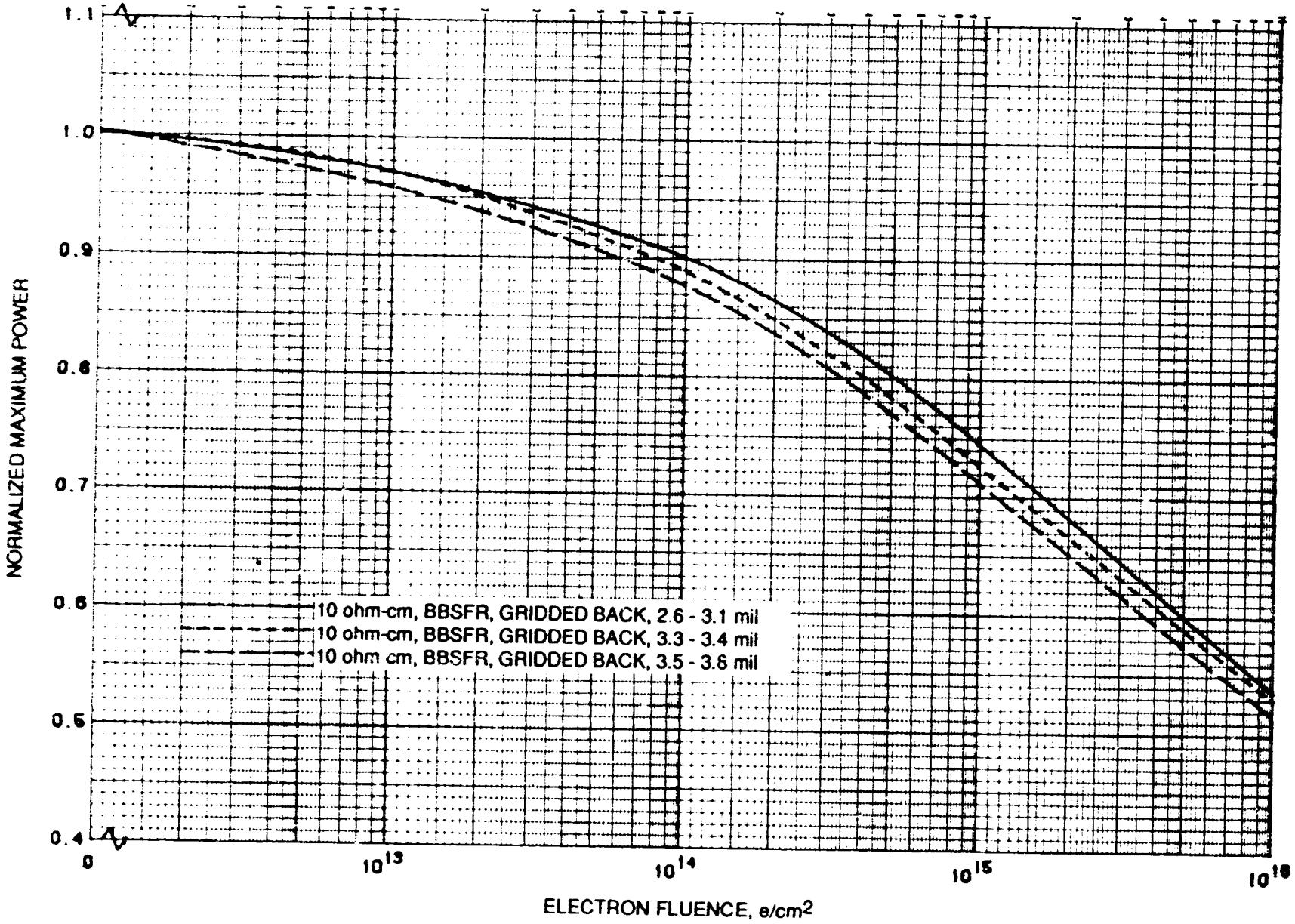

Figure 18. Normalized P_{max} vs. 1 MeV Electron Fluence for Si 10 ohm-cm BSFR Thin Cells (2.6 - 3.1 mils)

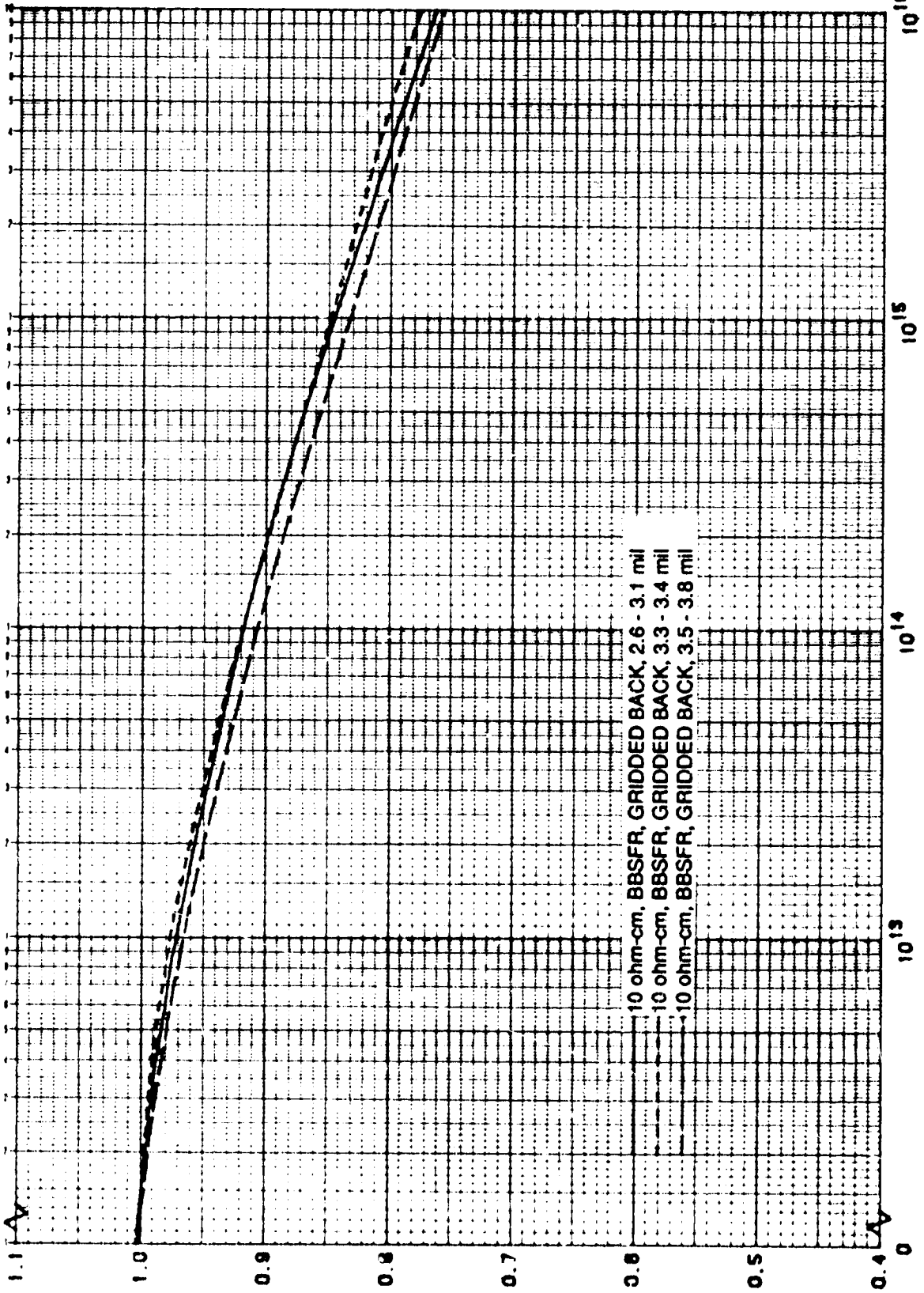

Figure 19. Normalized V_{mp} vs. 1 MeV Electron Fluence for Si 10 ohm-cm BSFR Thin Cells (2.6 - 3.1 mils)

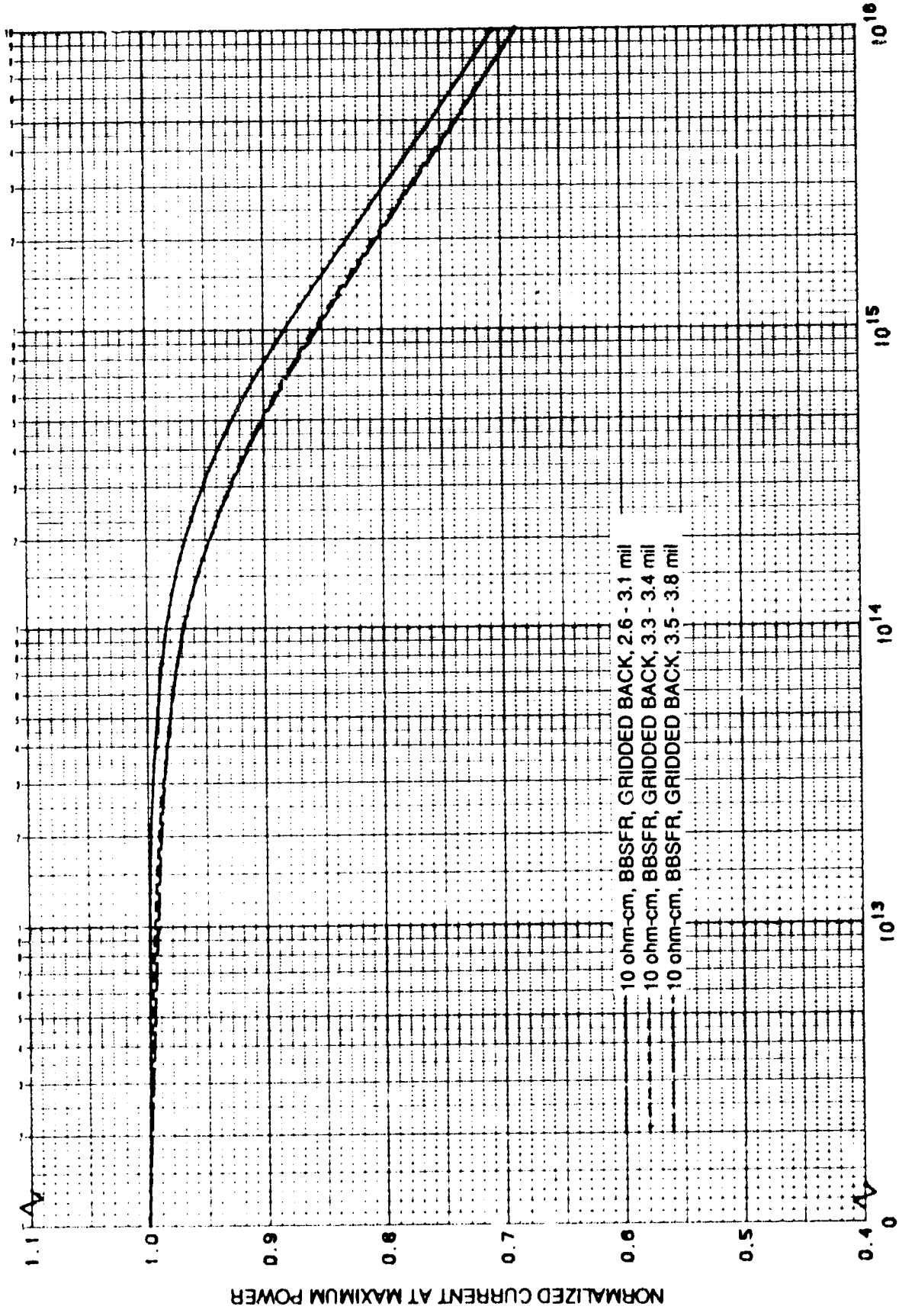

Figure 20. Normalized I_{mp} vs. 1 MeV Electron Fluence for Si 10 ohm-cm BSFR Thin Cells (2.6 - 3.1 mils)

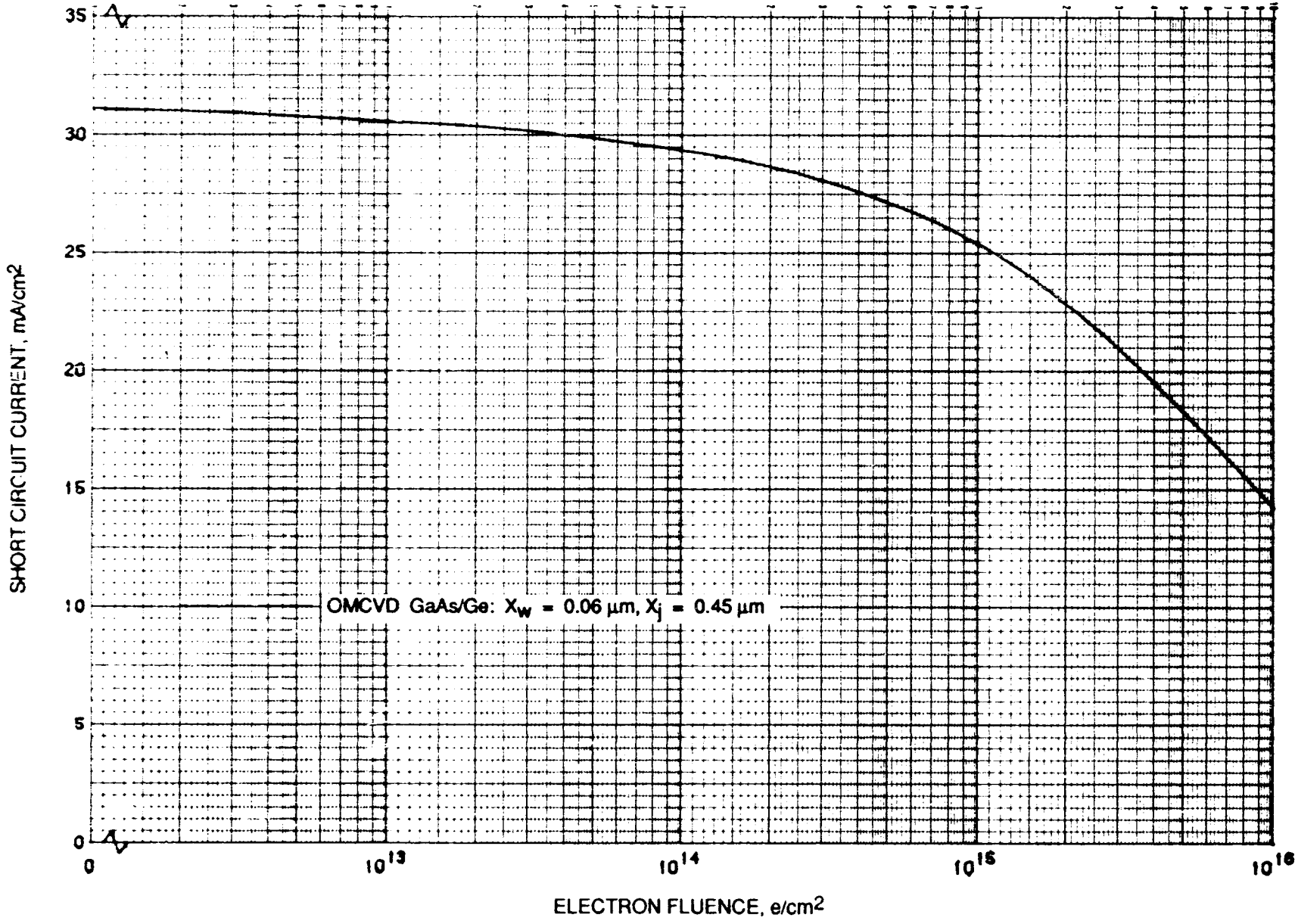

Figure 21. I_{sc} vs. 1 MeV Electron Fluence for GaAs/Ge Solar Cells

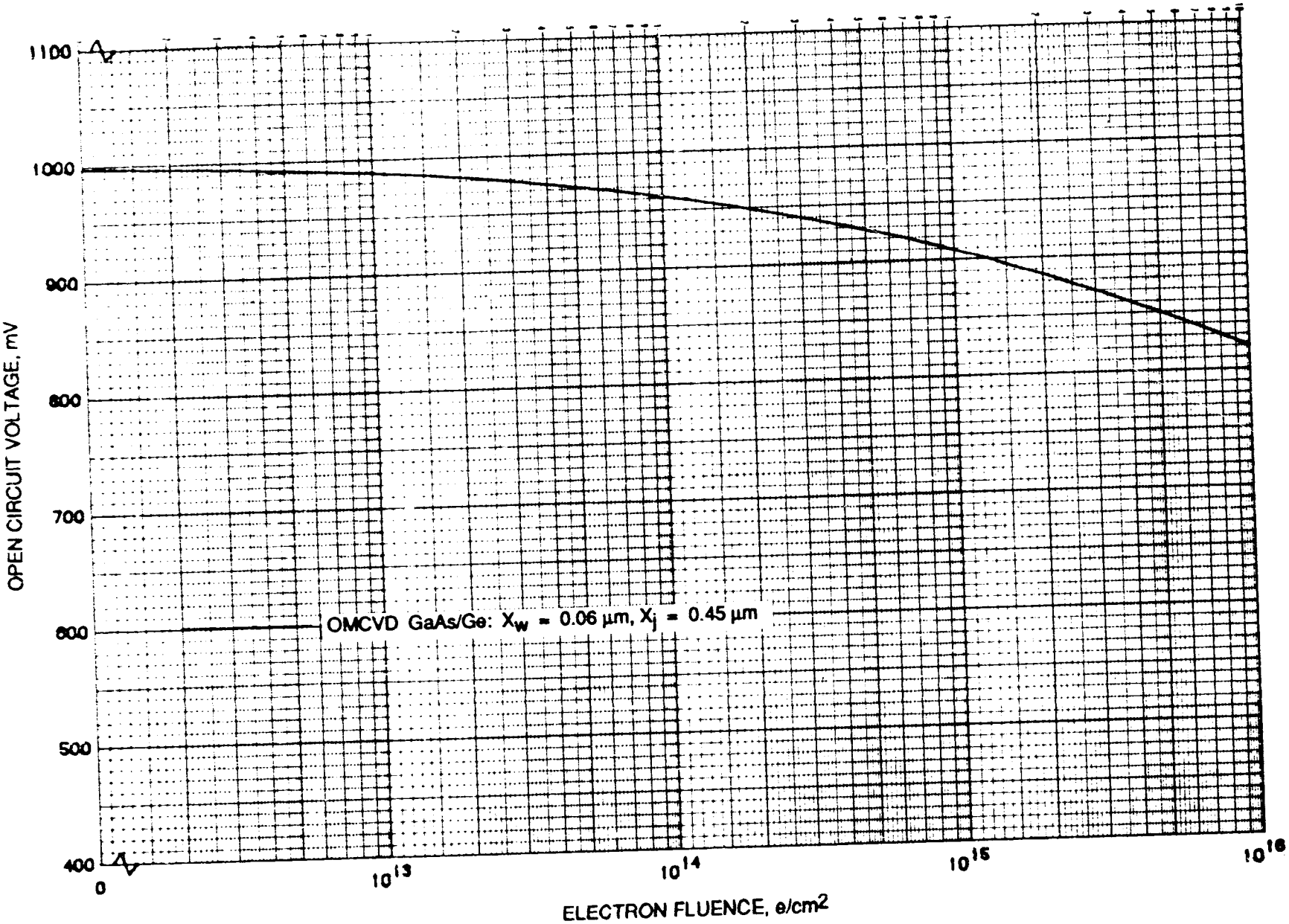

Figure 22 V_{oc} vs. 1 MeV Electron Fluence for GaAs/Ge Solar Cells

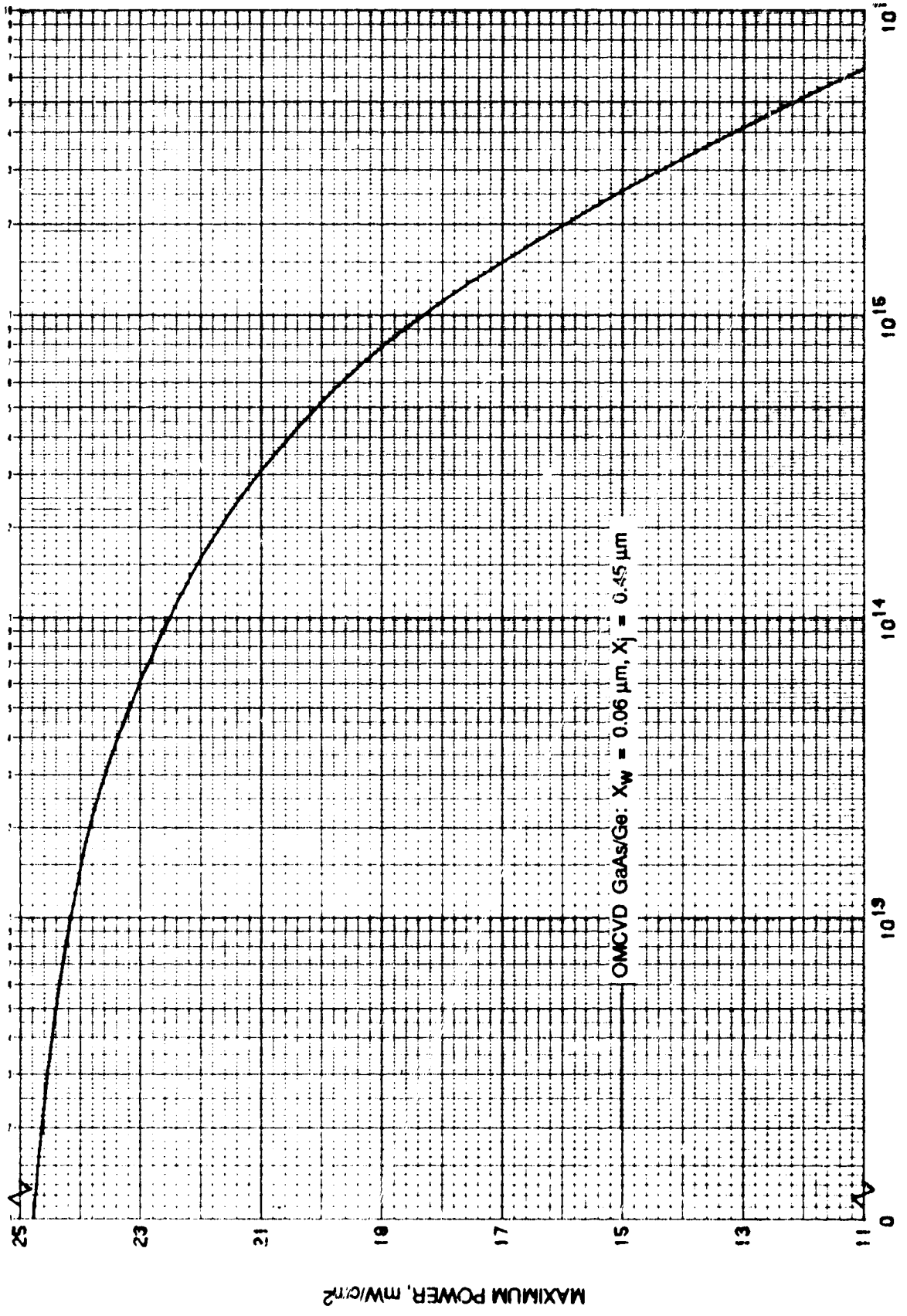

Figure 23. P_{max} vs. 1 MeV Electron Fluence for GaAs/Ge Solar Cells

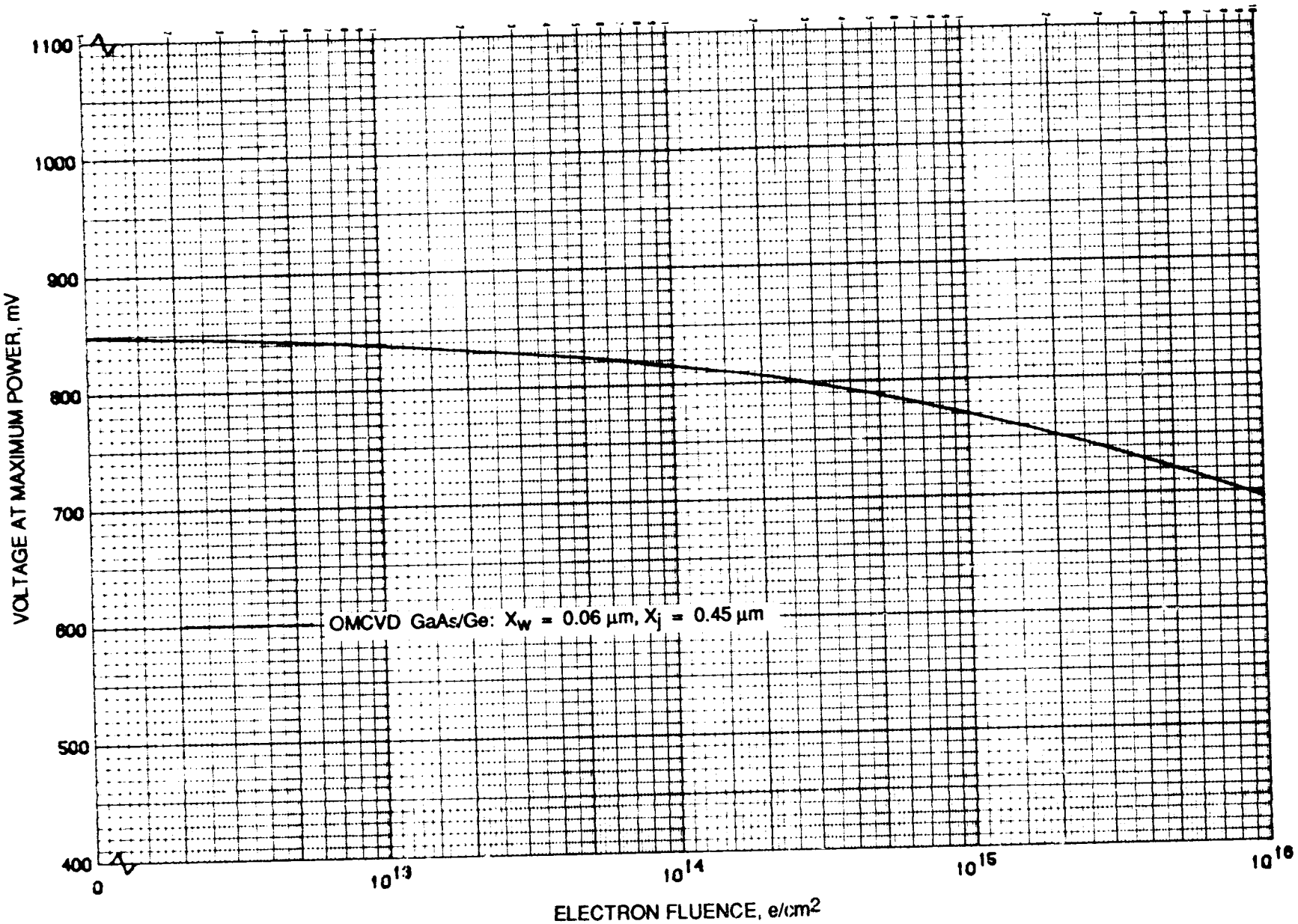

Figure 24. V_{mp} vs. 1 MeV Electron Fluence for GaAs/Ge Solar Cells

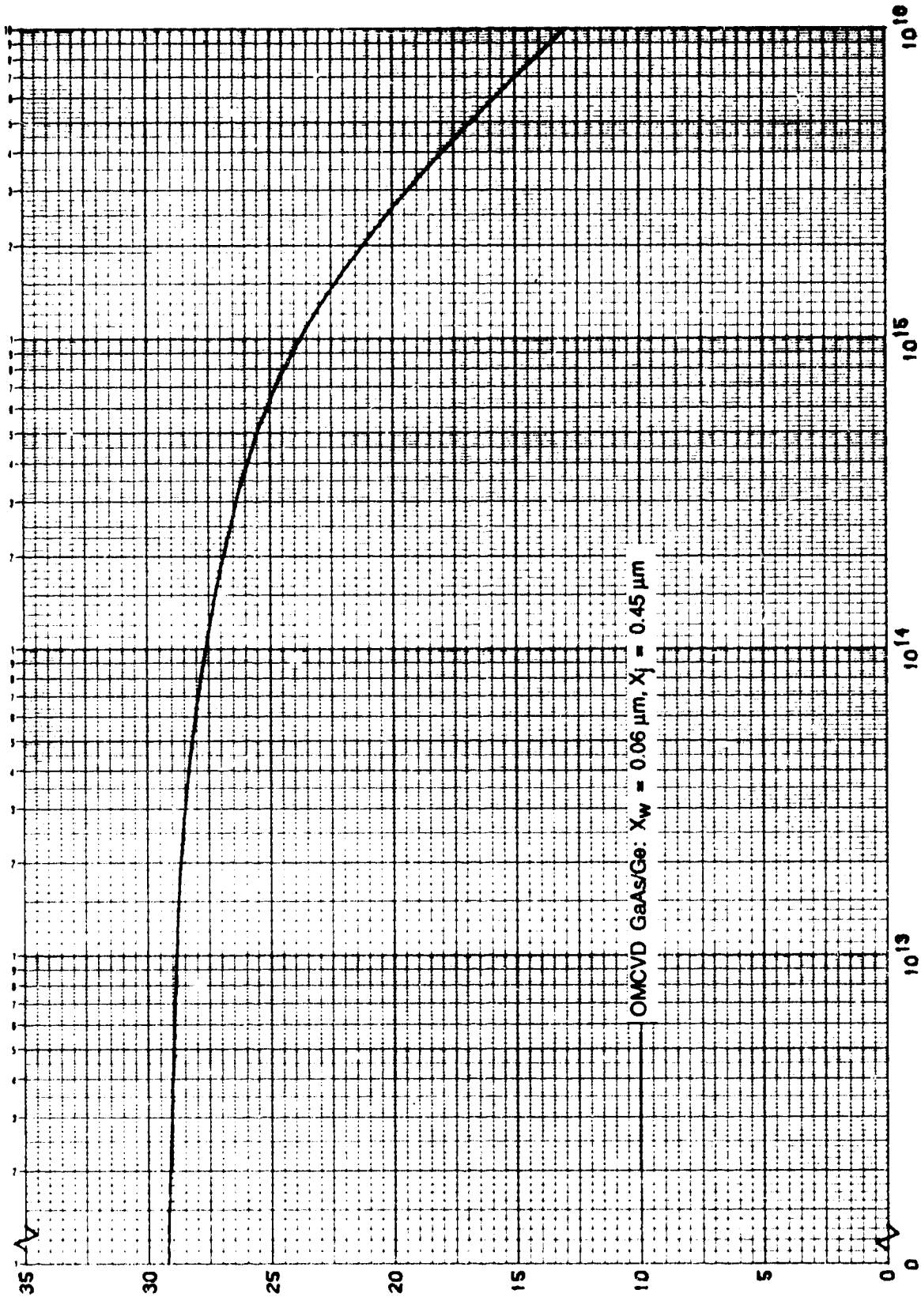

Figure 25. I_{mp} vs. 1 MeV Electron Fluence for GaAs/Ge Solar Cells

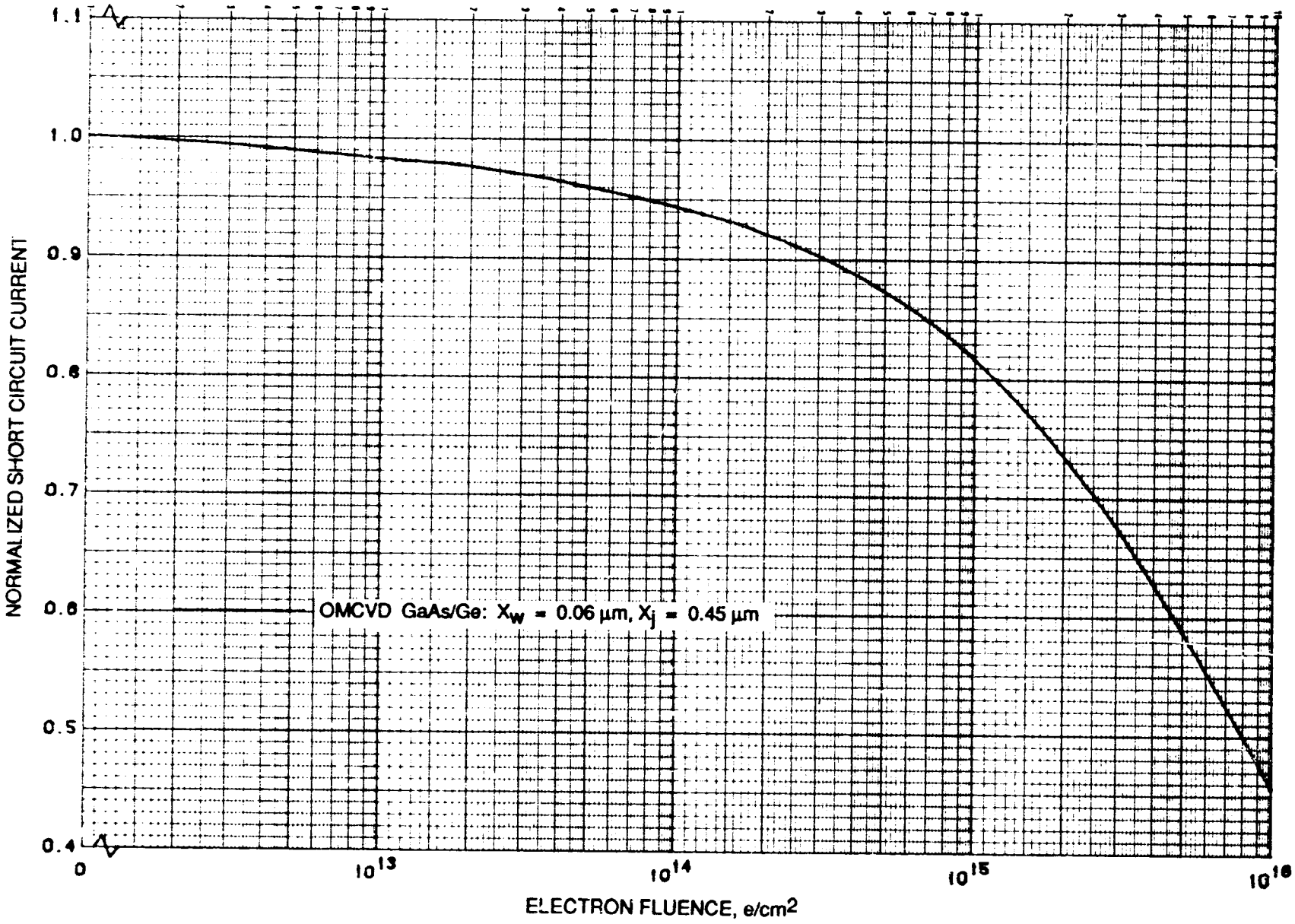

Figure 26. Normalized I_{sc} vs. 1 MeV Electron Fluence for GaAs/Ge Solar Cells

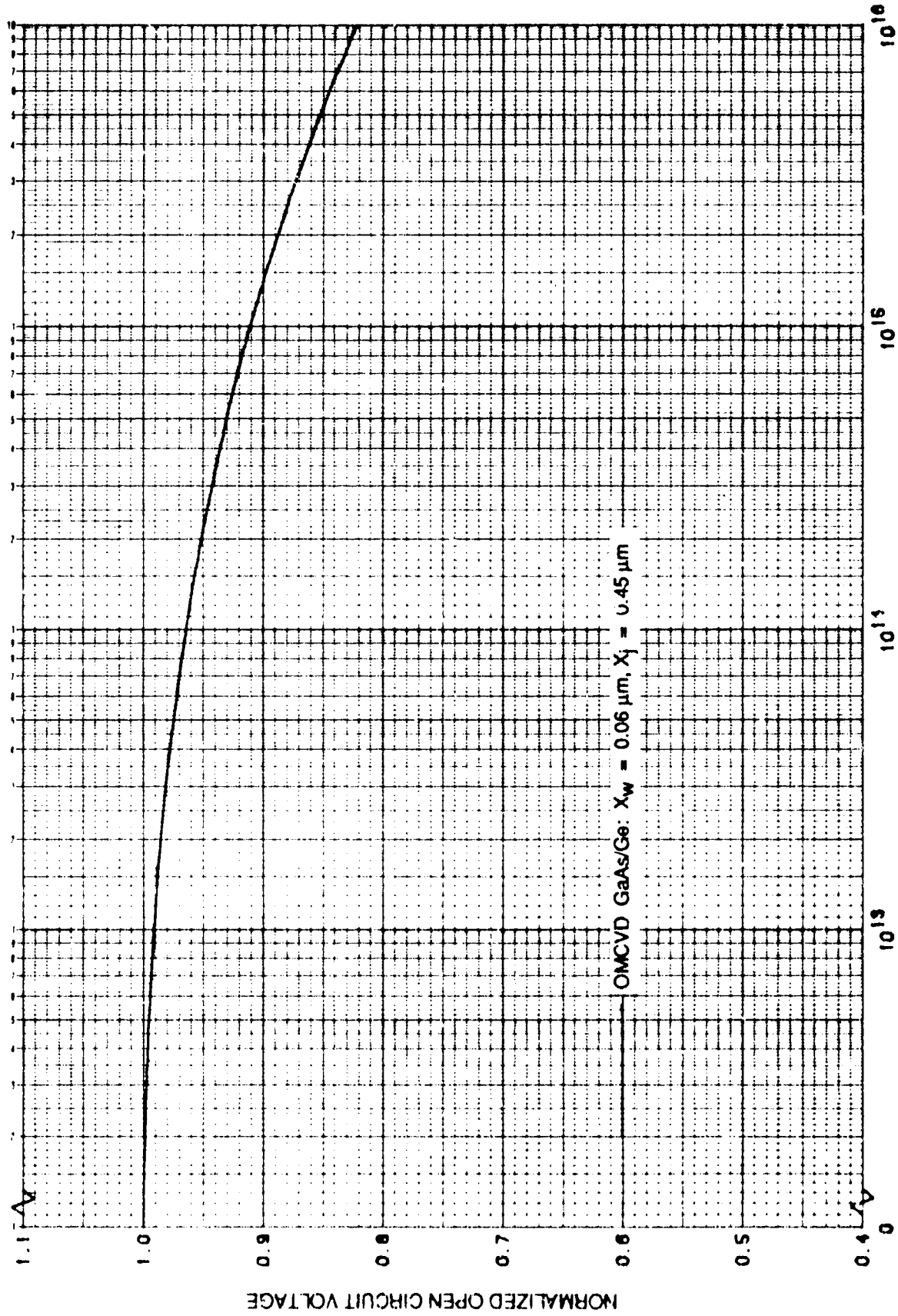

Figure 27. Normalized V_{oc} vs. 1 MeV Electron Fluence for GaAs/Ge Solar Cells

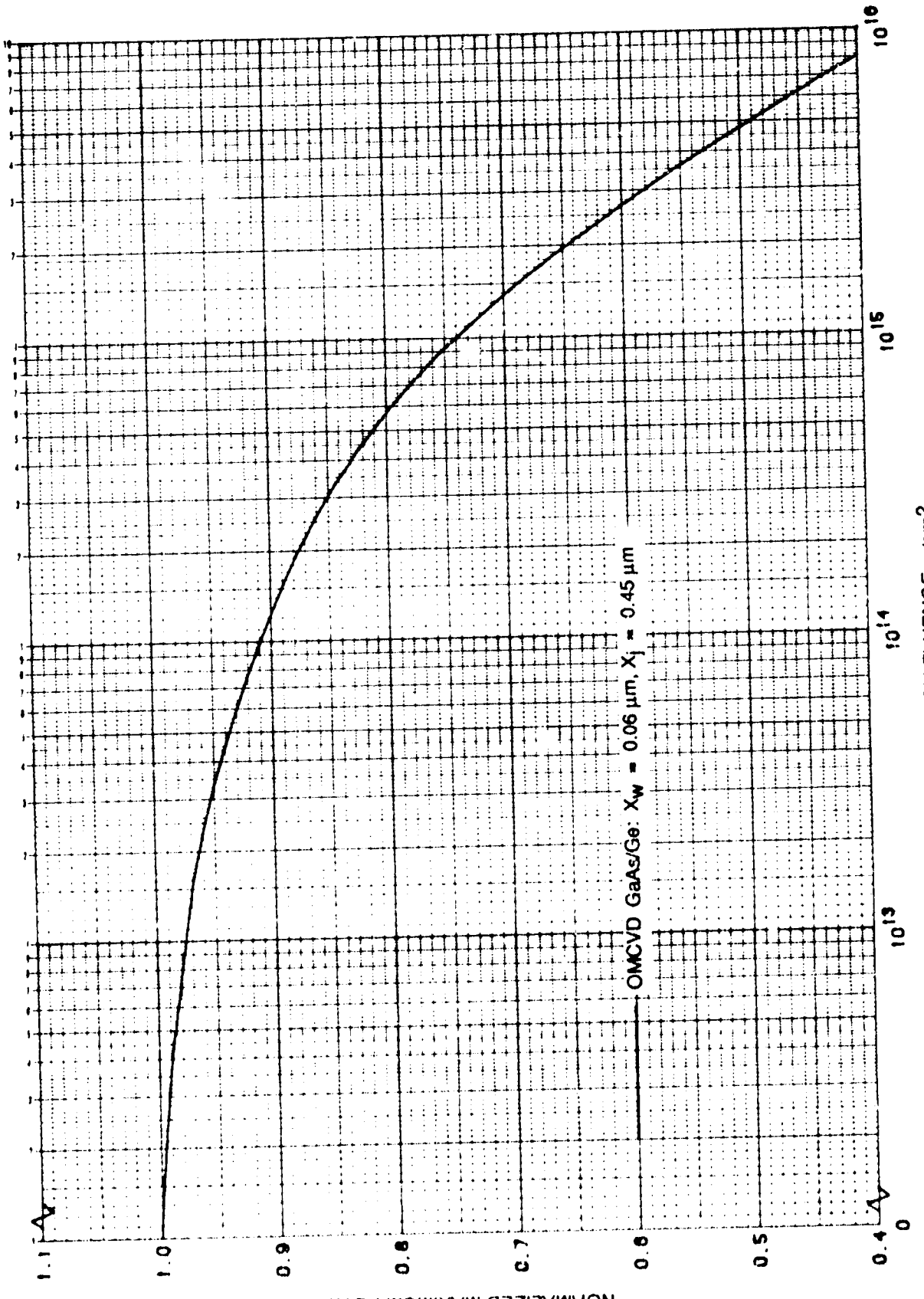

Figure 28. Normalized P_{max} vs. 1 MeV Electron Fluence for GaAs/Ge Solar Cells

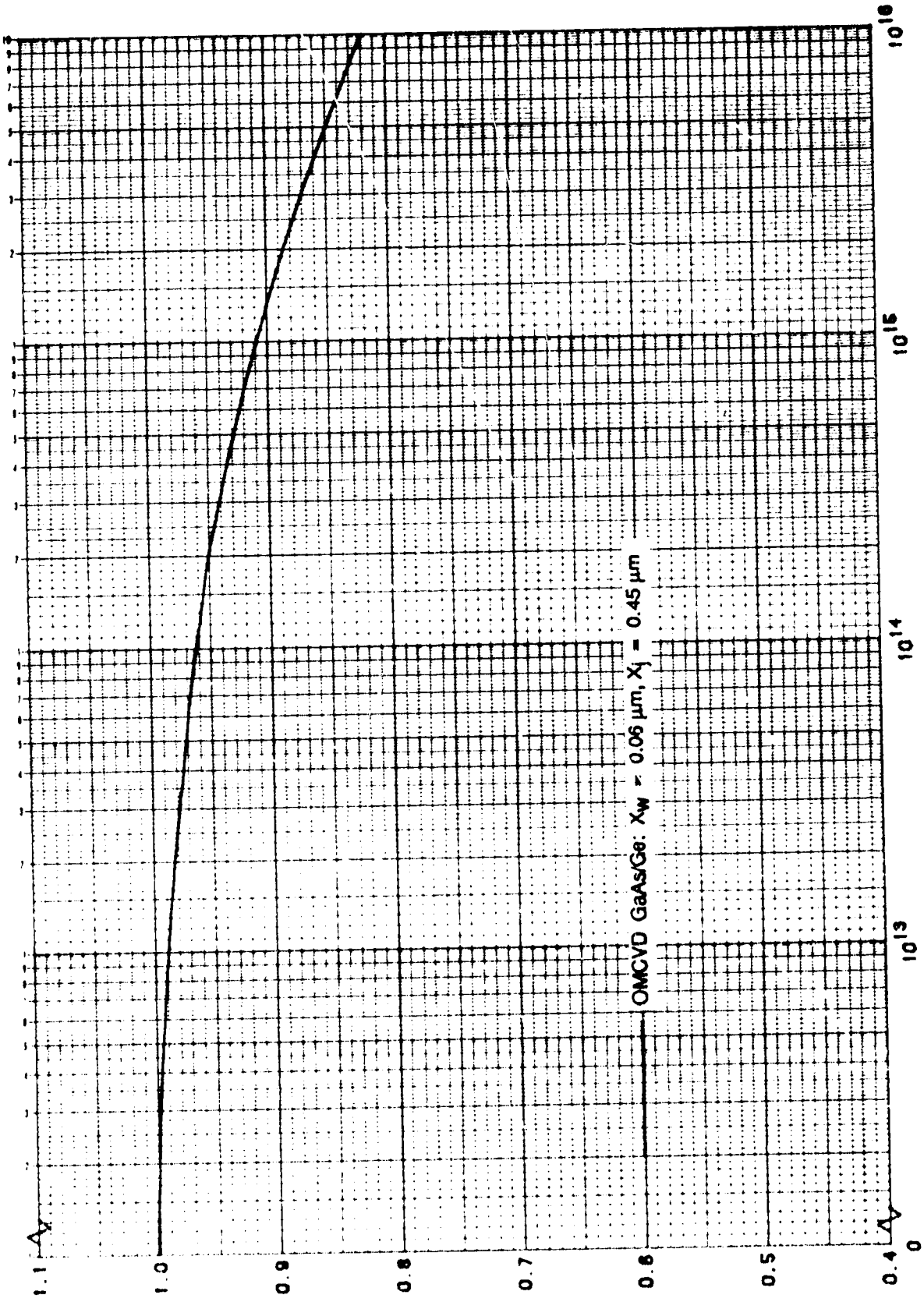

Figure 29. Normalized V_{mp} vs. 1 MeV Electron Fluence for GaAs/Ge Solar Cells

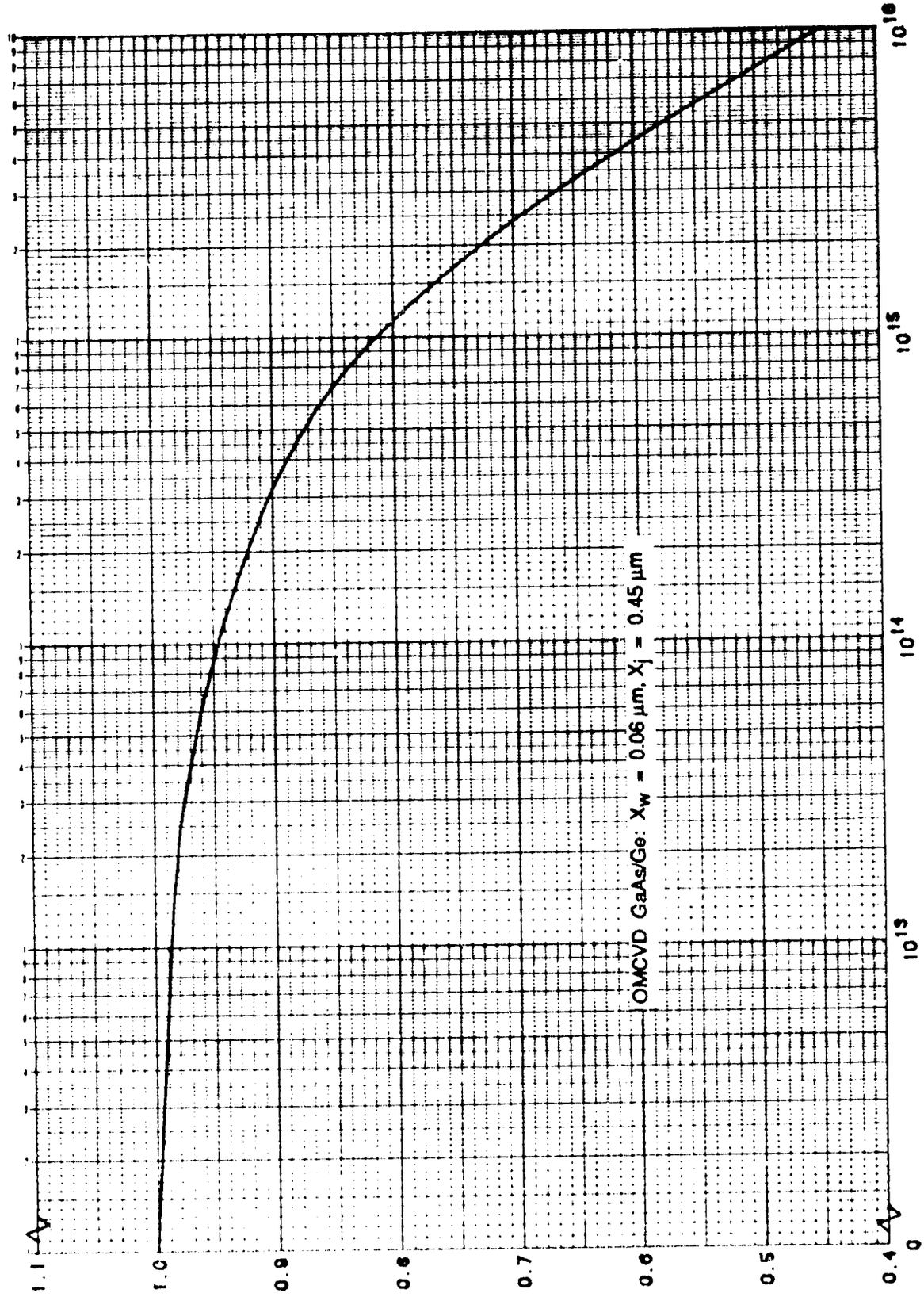

Figure 30. Normalized I_{mp} vs. 1 MeV Electron Fluence for GaAs/Ge Solar Cells

TECHNICAL REPORT STANDARD TITLE PAGE

1. Report No. JPL Pub 82-69 Addendum 1	2. Government Accession No.	3. Recipient's Catalog No.
4. Title and Subtitle Solar Cell Radiation Handbook Addendum 1: 1982-1988		5. Report Date Feb 15, 1989 6. Performing Organization Code
7. Author(s) Bruce Anspaugh		8. Performing Organization Report No. JPL Pub 82-69, Addendum 1
9. Performing Organization Name and Address JET PROPULSION LABORATORY California Institute of Technology 4800 Oak Grove Drive Pasadena, California 91109		10. Work Unit No. 11. Contract or Grant No. NAS7-918 13. Type of Report and Period Covered JPL Publication
12. Sponsoring Agency Name and Address NATIONAL AERONAUTICS AND SPACE ADMINISTRATION Washington, D.C. 20546		14. Sponsoring Agency Code

15. Supplementary Notes

16. Abstract

This is the first in a series of updates to the Solar Cell Radiation Handbook (JPL Publication 82-69). In order to maintain currency of solar cell radiation data, recent solar cell designs have been acquired, irradiated with 1 MeV electrons, and measured. The results of these radiation experiments are reported in this publication.

17. Key Words (Selected by Author(s)) Spacecraft Propulsion and Power Power Sources	18. Distribution Statement Unlimited/Unclassified		
19. Security Classif. (of this report) Unclassified	20. Security Classif. (of this page) Unclassified	21. No. of Pages	22. Price

END

DATE

FILMED

OCT 16 1989